

**FAILURE FORECAST OF BOEING 737 BLEED
AIR SYSTEM USING ARTIFICIAL NEURAL
NETWORKS**

BY

WAHEED AL-WADIEE

A Thesis Presented to the
DEANSHIP OF GRADUATE STUDIES

KING FAHD UNIVERSITY OF PETROLEUM & MINERALS
DHAHRAN, SAUDI ARABIA

In Partial Fulfillment of the
Requirements for the Degree of

MASTER OF SCIENCE

In

AEROSPACE ENGINEERING

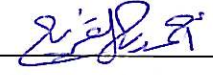
MUHARRAM 1433
DECEMBER 2011

KING FAHD UNIVERSITY OF PETROLEUM & MINERALS
DHAHRAN 31261, SAUDI ARABIA
DEANSHIP OF GRADUATE STUDIES

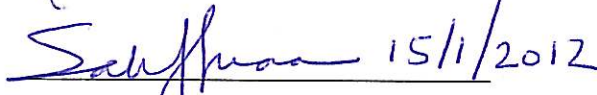
This thesis, written by **WAHEED AL-WADIEE** under the direction of his thesis advisor and approved by his thesis committee, has been presented to and accepted by the Dean of Graduate Studies, in partial fulfillment of the requirements for the degree of **MASTER OF SCIENCE IN AEROSPACE ENGINEERING**.

Thesis Committee


Dr. Wael G. Abdelrahman (Advisor)

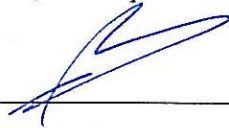

Dr. Ahmed Z. Al-Garni (Co-Advisor)


Dr. Prasetyo Edi (Member)

 15/1/2012
Dr. Salih Q. Duffuaa (Member)

 15/1/2012
Dr. Mohammad A. Abido (Member)


Dr. Ahmed Z. Al- Garni
Chairman, AE department


Dr. Salam A. Zummo
Dean of Graduate Studies



30/4/12
Date

ACKNOWLEDGEMENTS

“In the name of Allah, The Most Gracious and The Most Merciful”

Read, in the name of the lord and Cherisher, Who created man from a [leech-like] clot. Read, and the Lord is Most Bountiful, He Who taught [the use of] the pen, taught man that which he know not. Nay, but man doth transgress all bounds. In that he looked upon himself as a self-sufficient. Verily, to thy lord is the return [of all]. “(The Holy QURAN, Surah No.96).

Above and first of all, I thank and pray to Allah for His guidance and protection throughout my life, including the years of this study. I feel privileged to glorify His name in the sincerest way throughout this small accomplishment. And secondary my peace upon His Prophet, MOHAMMED (peace be up on him).

This study was carried out at the King Fahd University of Petroleum & Minerals, Dhahran, Saudi Arabia. The author is grateful for support provided.

It is a pleasure to give due acknowledgement to Dr. Wael G. Abdelrahman for his ready advice and unfailing support and for suggesting this useful problem as an M.S. thesis proposal. His able guidance and encouragement throughout the course of this study, which made this work possible, are deeply appreciated. I would also like to express my gratitude to the other members of the committee, especially Dr. Ahmad Z. Al-Garni, my co-advisor, for his assistance and guidance throughout this study, especially on providing me with his valuable previous work that includes the MATLAB code which is considered to be the backbone of my humble work.

TABLE OF CONTENTS

Acknowledgment.....	ii
List of Tables.....	vi
List of Figures.....	viii
Abstract.....	x
Arabic Abstract.....	xi
Chapter 1 INTRODUCTION.....	1
1.1 Bleed Air System Description.....	2
1.2 Bleed Air Regulator	3
1.3 High Stage Valve	4
1.4 Pressure Regulator and Shutoff Valve (PRSOV).....	7
1.5 Objectives.....	9
Chapter 2 LITERATURE REVIEW	10
2.1 Weibull.....	10
2.2 A.N.N.....	11
Chapter 3 WEIBULL METHODOLOGY.....	15
3.1 Weibull Regression Model (2 parameters).....	15
3.2 Bathtub Curve	17
3.3 Fitting the Weibull Model to the Data	19

3.3.1	Bleed Air Regulator (BAR-FH).....	19
3.3.2	Goodness-of-Fit Test (BAR-FH).....	24
3.3.3	Bleed Air Regulator (BAR-FC).....	27
3.3.4	High Stage Valve (HSV-FH).....	30
3.3.5	Goodness-of-Fit Test (HSV-FH).....	34
3.3.6	High Stage Valve (HSV-FC).....	36
3.3.7	Goodness-of-Fit Test (HSV-FC).....	39
3.3.8	Pressure Regulator and Shutoff Valve (PRSOV-FH).....	41
3.3.9	Goodness-of-Fit Test (PRSOV-FH).....	45
3.3.10	Pressure Regulator and Shutoff Valve (PRSOV-FC).....	46
3.3.11	Goodness of Fit Test (PRSOV-FC).....	50
Chapter 4	ANN METHODOLOGY.....	52
4.1	Artificial Neural Network.....	52
4.1.1	Introduction.....	52
4.1.2	Artificial Neural Networks Classifications.....	53
4.1.3	Sigmoid Activation Function.....	58
4.1.4	ANN Training Performance.....	59
4.1.5	Results and Discussion (Bleed Air Regulator-Flight Hour).....	60
4.1.6	Results and Discussion (Bleed Air Regulator- Flight Cycle).....	66
4.1.7	Results and Discussion (HSV-FH).....	71
4.1.8	Results and Discussion (HSV-FC).....	76

4.1.9	Results and Discussion (PRSOV-FH)	80
4.1.10	Results and Discussion (PRSOV-FC).....	84
4.1.11	Results Summary	88
Chapter 5	MODEL VALIDATION.....	91
Chapter 6	CONCLUSION AND FUTURE WORK.....	94
	REFERENCES.....	96
	Vitae.....	101

LIST OF TABLES

Table 3.1 Failure analysis for Bleed Air Regulator (FH)	21
Table 3.2 Regression Statistics (BAR-FH).....	22
Table 3.3 Statistics (BAR-FH).....	23
Table 3.4 KS GOF test for Bleed Air Regulator (FH).....	26
Table 3.5 BAR Weibull failure analysis (FC)	28
Table 3.6 Regression Statistics (BAR-FC).....	29
Table 3.7 Statistics (BAR-FC).....	29
Table 3.8 Failure analysis for High Stage Valve (FH)	31
Table 3.9 Regression Statistics (HSV-FH)	32
Table 3.10 Statistics (HSV-FH).....	33
Table 3.11 KS GOF test for High Stage Valve (FH).....	35
Table 3.12 High stage valve failure data (FC).....	37
Table 3.13 Regression Statistics(HSV-FC)	38
Table 3.14 Statistics (HSV-FC)	39
Table 3.15 KS test for high stage valve (FC).....	40
Table 3.16 PRSOV failure data (FH).....	42
Table 3.17 Regression Statistics (PRSOV-FH)	43
Table 3.18 Statistics (PRSOV-FH).....	44
Table 3.19 KS GOF test for PRSOV (FH)	45

Table 3.20 PRSOV failure data (FC).....	47
Table 3.21 Regression Statistics (PRSOV-FC)	48
Table 3.22 Statistics (PRSOV-FC)	49
Table 3.23 KS GOF test for PRSOV (FH)	50
Table 4.1 Bleed Air Regulator with different ANN structures (FH)	63
Table 4.2 Major network parameters	66
Table 4.3 Bleed air regulator with different ANN structures (FC)	67
Table 4.4 High bleed air regulator results percentage error (FC) compared to actual data	71
Table 4.5 High stage valve with different ANN structure (FH)	72
Table 4.6 High stage valve average percentage error (FH) compared to actual data	75
Table 4.7 high stage valve (cycles) with different ANN structures.....	76
Table 4.8 Stage valve average percentage error (FC) compared to actual data.....	79
Table 4.9 ANN results for PRSOV (FH)	80
Table 4.10 PRSOV analysis percentage error compared to actual data (FH).....	83
Table 4.11 ANN results for PRSOV (FC)	84
Table 4.12 PRSOV analysis percentage error compared to actual data (FC).....	87
Table 4.13 Results summary for all components (FH)	88
Table 4.14 Results summary for all components (FC)	89
Table 5.1 Partial data set for model verification.....	91

LIST OF FIGURES

Figure 1.1 Boeing 737 Bleed Air System	3
Figure 1.2 High Stage Valve and Regulator	6
Figure 1.3 High stage valve functional description	7
Figure 1.4 Pressure Regulator and Shutoff Valve (PRSOV).....	8
Figure 3.1 The Bathtub Curve	18
Figure 3.2 Weibull plot for failure data of Bleed Air Regulator (FH).....	22
Figure 3.3 Weibull plot for high stage valve (FT).....	32
Figure 3.4 Weibull plot for high stage valve (FC).....	38
Figure 3.5 PRSOV Weibull plot (FH)	43
Figure 3.6 PRSOV Weibull Plot (FC)	48
Figure 4.1 Simple Perceptron	55
Figure 4.2 Working Flow Chart for the BP ANN process.....	55
Figure 4.3 ANN (2, 4, 1) configuration	57
Figure 4.4 ANN (3, 6, 1) configuration	58
Figure 4.5 Log-Sigmoid Function	59
Figure 4.6 BAR (FH) ANN (2, 4, 1) comparison with actual data and Weibull.	64
Figure 4.7 BAR (FH) ANN (4, 8, 1) comparison with actual and Weibull data	64
Figure 4.8 BAR (FH) ANN (3, 6, 1) comparison with actual and Weibull data	65
Figure 4.9 BAR (FH) ANN (4, 10, 1) comparison with actual and Weibull data	65

Figure 4.10 BAR ANN (2,4,1) compared to the actual (FC).....	68
Figure 4.11 BAR ANN (3,6,1) compared to actual (FC).....	69
Figure 4.12 BAR ANN (4,8,1) compred to actual (FC)	70
Figure 4.13 BAR ANN results compared to actual and Weibull (FC)	70
Figure 4.14 High stage valve (FH) ANN (2, 4, 1) compared to actual data	73
Figure 4.15 High stage valve (FH) ANN (3, 6, 1) compared to actual data	74
Figure 4.16 High stage valve (FH) ANN (4, 8, 1) compared to actual data	74
Figure 4.17 High stage valve (FH) ANN compared to actual and Weibull.....	75
Figure 4.18 High stage valve (FC) ANN (2,4,1) compared to actual data	77
Figure 4.19 High stage valve (FC) ANN (3,6,1) compared to actual data	78
Figure 4.20 High stage valve (FC) ANN (4,8,1) compared to actual data	78
Figure 4.21 High stage valve (FC) ANN compared to actual data and Weibull	79
Figure 4.22 PRSOV (FH) ANN (2,4,1) comparison with actual data	81
Figure 4.23 PRSOV (FH) ANN (3,6,1) comparision with actual data	82
Figure 4.24 PRSOV (FH) ANN (4,8,1) with actual data.....	82
Figure 4.25 PRSOV (FH) ANN compared with Weibull	83
Figure 4.26 PRSOV (FC) ANN (2,4,1) comparison with actual data	85
Figure 4.27 PRSOV (FC) ANN (3, 6, 1) comparison with actual data	86
Figure 4.28 PRSOV (FC) ANN (4,8,1) comparison with actual data	86
Figure 4.29 PRSOV ANN comparison with Weibull.....	87
Figure 5.1 BAR (FC) test sample.....	92

ABSTRACT

In this study, the failure rate of different types of bleed air control valves for the Boeing 737 aircraft is modeled. Two approaches are utilized to perform this work. In the first approach, Weibull model, in which different parameters are utilized and tested, is used. In the second one, a common type of the Artificial Neural Network (ANN) modeling is used. A Feed-forward back-propagation algorithm is implemented to train the network. Subsequently, the optimum number of neurons and layers that give the best result compared to the actual data are determined. Finally, the outputs from both models are compared against the actual data. The final results show a high level of accuracy of the ANN's predictions compared to the more traditional Weibull modeling. The developed verified model lends itself to applications that extend from scheduling replacements operations of these valves, to developing plans for inventory management in any aviation engines maintenance facility.

الخلاصة

الاسم : وحيد علي الوادعي

عنوان البحث: التنبؤ باعطال نظام الهواء في طائرات البوينج من طراز 737 باستخدام الشبكات العصبية الاصطناعية

التخصص: هندسة الطيران والفضاء

تاريخ الدرجة العلمية : محرم \ 1433 (ديسمبر 2011)

في هذا البحث تم تحليل وتنبؤ الاعطال لبعض الصمامات في نظام الهواء لطائرات البوينج 737 باستخدام طريقتين علميتين. في الطريقة الأولى , تم استخدام التحليل الوائيلي أما في الطريقة الثانية فتم استخدام الشبكات العصبية الاصطناعية. وللحصول على أدق النتائج, تمت دراسة وتحليل الشبكات العصبية وذلك بتغيير عدد الطبقات والأعصاب للشبكة خلال عملية المحاكاة للتنبؤ بالأعطال. أخيرا تمت مقارنة مخرجات البرنامج بالبيانات الفعلية لعدد مرات الأعطال. وبناء عليه, فقد إتضح خلال من خلال هذه المقارنة ان الشبكات العصبية الاصطناعية لديها القدرة الفائقة لمحاكاة النتائج الفعلية لعدد مرات الأعطال. وللزيادة في التحقق من دقة النتائج, تمت المقارنة مع مخرجات التحليل الوائيلي.

يمكن استخدام هذه الدراسة كأداة لتخطيط صيانة الصمامات المذكوره في هذه الدراسة من خلال معرفة عدد الوحدات المطلوب توفرها في مستودعات الصيانة كبديل في حالة الأعطال لأي صمام. يمكن قياس هذه الدراسة كإطار عام يمكن استخامه في أي مجال من مجالات الصيانة.

Chapter 1

INTRODUCTION

Calculating the age of any airplane's part is a vital process because it has a direct impact not only on the safety of the aircraft but also on the efficiency of any flight operations. The bleed air system is one of those systems that operate under extreme temperature and pressure conditions, a failure in such a system could cause a catastrophic damage to other aircraft systems. For example, a failure of the bleed air regulator could affect the pressurization system which might jeopardize the safety of the flight especially when cruising at high altitudes. Because of that, continuous monitoring and preventive maintenance are significant to enhance the aircraft reliability and safety especially during the critical phase of the flight (i.e., takeoff and landing).

During the last few years, a lot of efforts have been made on trying to forecast and predict the failure of equipment and systems using some traditional statistical models, but unfortunately these models sometimes do not give the best outcome due to the complexity and nonlinearity of the data gathered from many maintenance records. However, when it comes to airplanes, failure prediction analysis should be carefully conducted with an adequate level of accuracy in order to achieve highest levels of safety and efficiency and to avoid inaccurate interpretation and results that could lead to harmful consequences.

1.1 Bleed Air System Description

Since the 737 bleed air control valves are used as a test model to demonstrate the analysis method, it would be appropriate to introduce the function and layout of the system before proceeding with a description of our work. The basic idea of any aircraft bleed air system is to extract air from the engine and use that air to serve other systems. Engine bleed air is obtained from the 5th and 9th stages of the engine compressor section. When 5th stage low pressure bleed air is insufficient for the bleed air system requirements, the high stage valve modulates to open to maintain adequate bleed air pressure. During takeoff, climb, and most of the cruise conditions, low pressure bleed air from the 5th stage is sufficient and the high stage valve remains closed because the engine power settings at these phases of flights are generally high. The following systems rely on the bleed air system for operation:

- Air conditioning
- Pressurization system
- Engine starting
- Hydraulic reservoirs pressurization
- Water tank pressurization system

Figure 1.1 shows the basic layout of the Boeing 737 bleed air system [37].

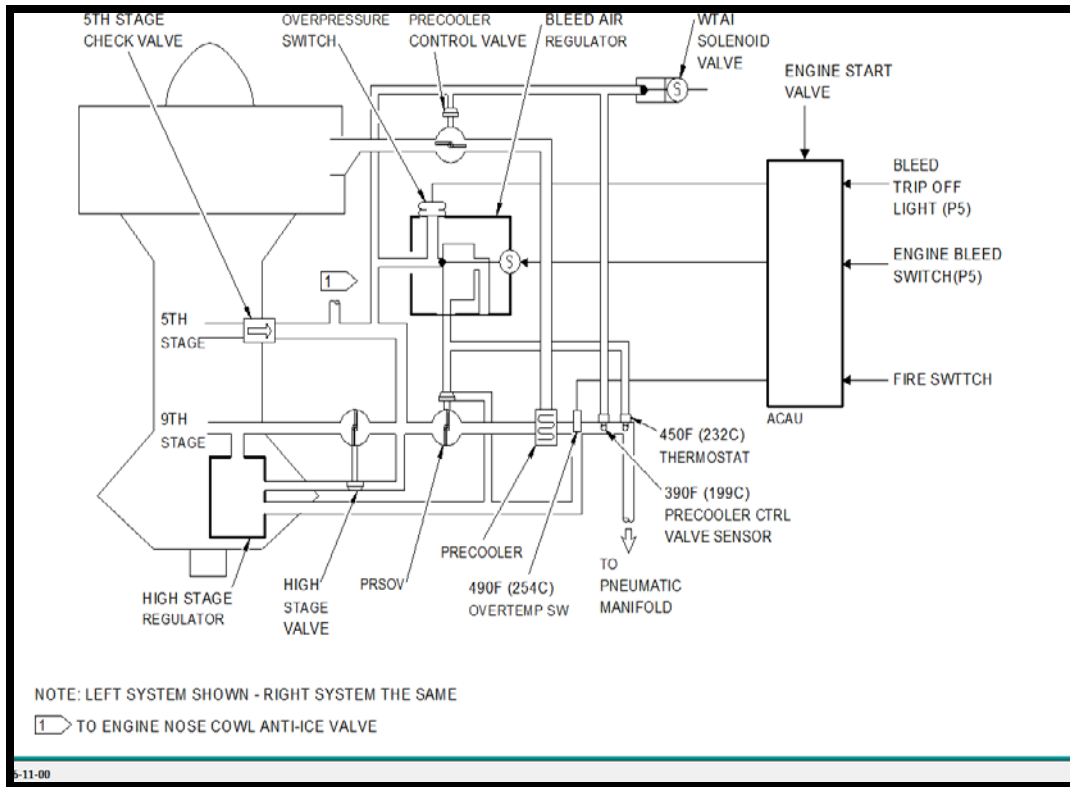


Figure 1.1 Boeing 737 Bleed Air System

1.2 Bleed Air Regulator (BAR)

The bleed air regulator is a pneumatic controller designed to provide regulated control pressure, with electrically controlled shutoff, from a bleed air source. Other functions incorporated are electrical indication of excessive bleed air supply pressure, automatic electrical shutoff of regulated control pressure in the event a separate downstream pressure exceeds bleed air supply pressure and a relief valve to maintain regulation of control pressure in the event of pressure regulator failure. The bleed air regulator controls the flow of engine bleed air to the pneumatic manifold. The bleed air regulators have

overpressure switches to prevent overpressure conditions and shutting the air-condition pack off.

1.3 High Stage Valve (HSV)

The high stage regulator and valve control the supply of high stage engine bleed air. The high stage regulator operates the high stage valve. The high stage valve controls the flow of bleed air from the 9th stage bleed air manifold. This valve works under extreme conditions in term of pressure and temperature, because of that, the reliability and maintainability of this valve was carefully designed in order to avoid any bleed control malfunctions.

The high stage regulator gets unregulated air from a tap on the 9th stage bleed air manifold. The unregulated air goes through the pneumatic shutoff mechanism to the reference pressure regulator. The reference pressure regulator decreases the pressure to a constant control pressure. A relief valve prevents damage to the high stage valve if the reference pressure regulator fails. The control pressure from the high stage regulator goes to chamber A of the high stage valve. The actuator opens the valve against spring force and pressure in chamber B. The combination of forces that operate on the actuator cause the valve to regulate the downstream pressure to 32 psi (nominal). During normal operation, the high stage valve closes for these reasons:

- 1) Downstream pressure is more than 9th stage pressure.
- 2) The 5th Stage pressure is greater than the high stage regulated pressure.

When downstream pressure is more than 9th stage pressure, the reverse flow mechanism in the high stage regulator opens and bleeds off the control pressure to the high stage valve. The high stage valve then closes. When 5th stage manifold pressure is greater than the high stage regulated pressure (nominal 34 psi), the high stage valve closes because the force in chamber B, combined with the spring force, is greater than the force in chamber A. This causes the high stage valve to close. The pneumatic shutoff mechanism increases the life of the high stage regulator. The shutoff operates after the shift to 5th stage engine supply occurs. High pressures (110 psi) in the supply port operate a shutoff mechanism. The shutoff mechanism closes the supply to the regulator inlet and vents the regulator.

This reduces the duty cycle of the regulator and exposure to extreme pressures and temperatures during high engine power operation. A relief valve in the high stage valve decreases downstream pressure in the inter stage duct when the pressure regulator and shutoff valve (PRSOV) is closed.

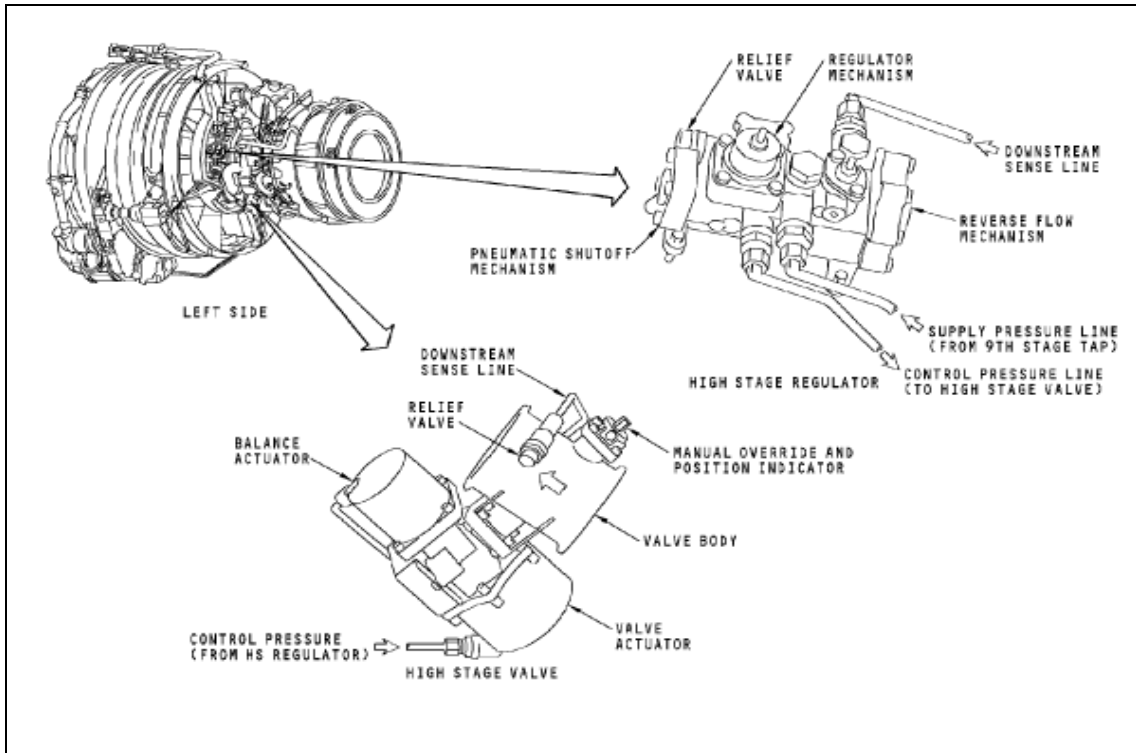


Figure 1.2 High Stage Valve and Regulator

Figure 1.2 and Figure 1.3 shows the high stage valve with a detailed schematic about the functional description [37].

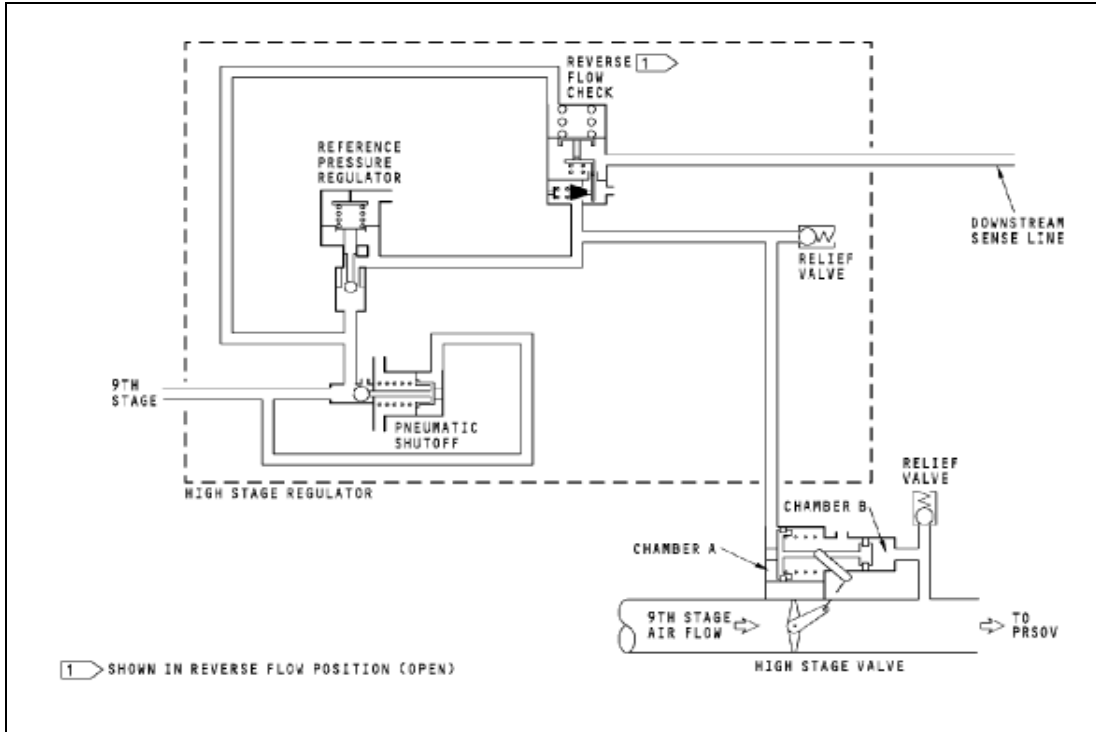


Figure 1.3 High stage valve functional description

1.4 Pressure Regulator and Shutoff Valve (PRSOV)

A bleed air regulator and the pressure regulator and shutoff valve (PRSOV) control the flow of bleed air to the pneumatic manifold. The bleed air regulator (BAR) operates the pressure regulator and shutoff valve (PRSOV). The PRSOV is pneumatically controlled by the BAR.

These are the PRSOV control functions.

- a. Shutoff of engine bleeds air
- b. Pressure regulation of engine bleeds air (42 psi nominal)

- c. Temperature limitation of engine bleeds air (450F/232C)

The PRSOV is a butterfly valve that is spring-loaded closed. The valve has these parts:

- 1- Pneumatic actuator.
- 2- Manual override and position indicator.
- 3- Control air port.
- 4- Downstream sense port.

Figure 1.4 shows the PRSOV with its main components [37].

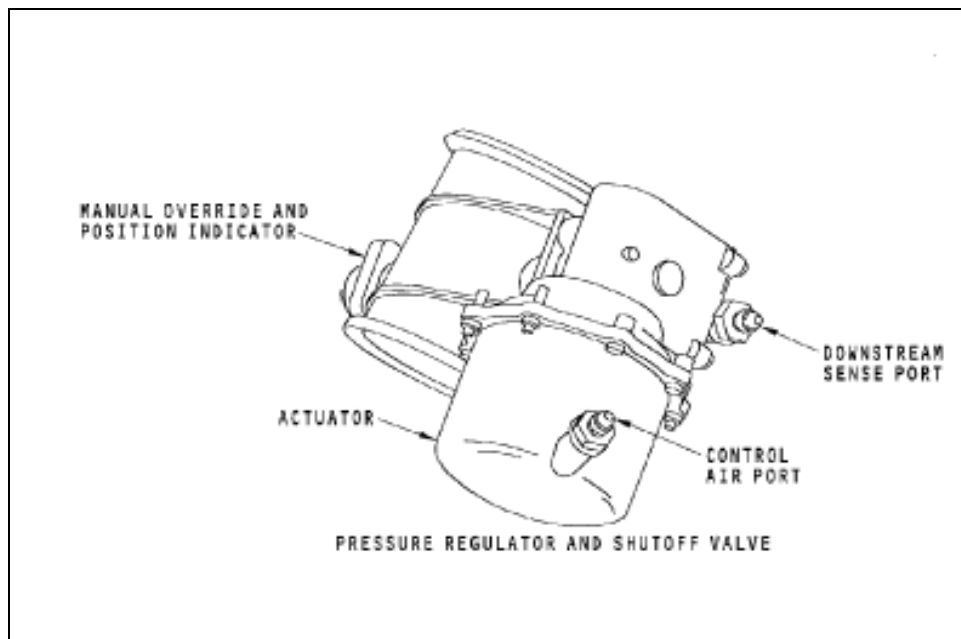


Figure 1.4 Pressure Regulator and Shutoff Valve (PRSOV)

1.5 Objectives

The main objective of this study is to design an Artificial Neural Network model that can predict the failure of some bleed air system components of an aircraft based on a history of data collected from a maintenance facility. The effect of multiple ANN configurations on the accuracy of the network performance is extensively discussed in order to come up with an optimum structure that has the ability to ensure a reliable data which can be utilized for maintenance planning. Another objective is to conduct full analysis for the Weibull model. Finally, both results will be compared to confirm the reliability of each model.

Chapter 2

LITERATURE REVIEW

2.1 Weibull Distribution

The history of the Weibull distribution can be traced back to 1928, when two researchers, Fisher and Tippett, deduced the distribution in their study of the extreme value theory. In the late 1930s, a Swedish professor Waloddi Weibull derived the same distribution and his hallmark paper in 1951 made this distribution fashionable [1]. In his paper Professor Weibull explained the reasoning of the Weibull distribution through the phenomena of the weakest link in the chain, [2].

Weibull analysis is widely used in failure prediction modeling in many fields. It is considered to be one of the most widely used distributions in reliability data analysis. Many methods have been proposed for estimating the two Weibull parameters, among which Weibull probability plot (WPP), maximum likelihood estimation (MLE) and least squares estimation (LSE) are the methods frequently used nowadays. Zaretsky proposed a generalized Weibull-based methodology for structural life prediction that uses a discrete-stressed - volume approach. They applied this methodology to qualitatively predict the life of a rotating generic disk with circumferentially placed holes as a function of the various Weibull parameters [3].

Al-Garni studied the failure rate in many aviation industry fields with a focus on aircraft components and systems by using both two and three parameters Weibull [4-13]. His new

approach was to study and calculate the reliability analysis not only on the component level, but also at the system level. Phased Bi-Weibull, mixture model were used to estimate the parameters in their study. Through his study, he focused on a lot of maintenance issues and procedures that would promote and enhance the reliability of studied system by concluding his researches with some practical recommendation related to the maintenance practices and inventory systems to avoid an under or over stock parts.

Shaikh [14] studied the reliability of some rotating equipment that is used in oil and gas field, two parameters Weibull was utilized at the study. Smaha studied the utilization of Weibull to predict the failure of some equipment based on history of data to give an indication of the component failure mechanism, [15]. He has also demonstrated that Weibull could be utilized in calculating the number of future failures according to the mean time between failures (MTTF). Erwin with assistance from NASA used Weibull model in aging and predicting the life of aircraft engine structures including critical rotating components like high pressure turbine blades, fan, and compressors, [16]. Lewis used regression based analysis which will be basically used in this study [17-18].

2.2 Artificial Neural Network (A.N.N)

McCulloch and Pitts tried to understand how the brain could produce highly complex patterns by using many basic cells that are connected together. They formed a logical calculus of neural network, [19]. A network consists of number of neurons and properly set synaptic connections that can compute any computable function. A simple logic function is performed by a neuron in this case based upon on the weights set in the McCulloch-Pitts neuron. The arrangement of neuron in his case maybe represented as a

combination of a logic function. The most important type feature of this type of neuron is the concept of the threshold. When the net input to a particular neuron is greater than the specified threshold by the user, the neuron fires. Logic circuits are found to use this type of neuron extensively.

Later, in Hebb's book, an explicit statement of a physiological learning rule for synaptic modification was presented for the first time [20]. Hebb proposed that the connectivity of the brain is continually changing as an organism learns differing functional tasks, and that neural assemblies are created a change. The concept behind the Hebb theory is that if two neurons are found to be active simultaneously the strength of connection between the two neurons should be increased. The concept is similar to that of correlation matrix learning. Moreover, Rosenblatt introduced perceptions. In perceptions network the weights on the connection paths can be adjusted.

A method of iterative weight adjustment can be used in perception net [21]. The perception net is found to converge if the weights obtained allow the net to produce exactly all the training inputs and target output vector pairs. Later, Widrow and Hoff introduced (ADALINE), abbreviated from Adaptive Linear Neuron uses a learning rule called as Least Mean Square (LMS) rule or Delta rule [22]. This rule is found to adjust the weights so as to reduce the difference between the net input to the output and the desired output. The convergence criteria in this case are the reduction of mean square error to a minimum value. This delta rule for a single layer can be called a precursor of the back propagation net used for multi-layer nets. The multi-layer extension of Adaline formed the Madaline.

In 1982, John Hopfield's introduced new concept networks, Hopfield showed how to use "Using spin glass" type of model to store the information in dynamically stable networks, [23]. His work paved the way for physicists to enter neural modeling, thereby transforming the field of neural networks.

Three years later, Parker back propagation net paved its way into neural networks, [24]. This method propagates the error information at the output units back to the hidden units using generalized delta rule. This net is basically a multilayer, feed foreword net trained by means of back propagation. Back propagation net emerged as the most popular learning algorithm for the training for multilayer perceptions and has been the workhouse for many neural network applications. This approach became common in modeling engineering and industrial problems. As a result Broomhead and Lowe developed Radial Based Functions (RBF). This is also a multilayer net that is quiet similar to the back propagation net. Al-Garni utilized the back propagation approaches to predict the failure of some equipment, [4-13]. The network topology and architecture played a significant role in the accuracy of the prediction. Selecting the right structure of the network was one the challenges in the study in order to come up with an optimum model with good parameters that would lead to a reliable prediction of the failure.

Kutsurelis utilized ANNs as a forecasting tool to study their ability in predicting the trend of some stock markets indices, [25]. Accuracy of the back propagation algorithm which was used to train the network was compared against a traditional forecasting method and multiple linear regression analysis. From his study, it was concluded that neural networks do have the capability to forecast financial markets and, if

properly trained, the individual investor could benefit from the use of this forecasting tool.

Soumitra proposed a model that could be implemented at aircraft maintenance, repair, and overhaul (MRO), [26]. He focused on many applications that could be facilitated by the artificial neural network. His main concept was to feed all the aircraft original equipment manufacturer manual (OEM) data to the network. By doing so, the probability at the point and the extent of damage caused in an aircraft with a better accuracy can be predicted.

Abd Kadir used ANN to calculate and predict the remaining useful life (RUL) of rotating machinery, [27]. He implemented his study on bearings life by utilizing Feed Forward neural network (FFNN), the study compared results from both ANN and Weibull model with a conclusion of better prediction analysis from the artificial neural network model.

The accuracy of ANN predictions to critical aircraft engine components has not been adequately investigated yet. In the present work, an initial modeling of failure rates using Weibull approach will first be introduced. Then a feed forward back propagation algorithm will be implemented to predict the engine valves using collected data corresponding to five years of operation in an aviation facility. The effect of model parameters will be investigated and its accuracy will be verified. Both flight hours and flight cycles will be used in failure data representation to give flexibility in maintenance scheduling. Finally possible operational applications of the developed model will be presented.

Chapter 3

WEIBULL METHODOLOGY

3.1 Weibull Regression Model

The Weibull model is one of the most commonly used models to identify the failure characteristics of any component parts. In aerospace, it is considered to be one of the sophisticated tools that are widely utilized in order to identify unexpected failures for some parts. It also gives an optimum maintenance strategy, especially when researchers try to estimate the remaining age for any parts with increasing failure. The beauty about this model is the ability to provide reasonably accurate failure analysis and failure predictions with relatively small sample of data. This means that it is possible to use data as the first failure emerges and decide on corrective actions before more failure data is generated.

There are many models for the Weibull distribution like the three parameters model, mixture model and phase-bi model which could be implemented due to the nature of the study. In this study the two parameters model will be used. The Weibull failure distribution may be used to model both increasing and decreasing failure rates. It is characterized by a hazard rate function $\lambda(t)$ of the form:

$$\lambda(t) = at^b$$

which is a power function. The function $\lambda(t)$ is increasing for $a > 0, b > 0$ and is decreasing for $a > 0, b < 0$. For mathematical convenience it is better to express the hazard function $\lambda(t)$ in the following form to better emphasize the physics of the modeling process:

$$\lambda(t) = \frac{\beta}{\eta} \left(\frac{t}{\eta} \right)^{\beta-1} \quad \eta > 0, \beta > 0, t \geq 0 \quad (3.1)$$

The reliability function $R(t)$ which indicates the probability of surviving beyond a given time t can be derived from the failure rate function as follows:

$$R(t) = \exp \left[- \left(\frac{t}{\eta} \right)^\beta \right] \quad (3.2)$$

The cumulative distribution function $F(t)$ which indicates the probability that a failure occur before time t can be defined as the following:

$$F(t) = 1 - R(t)$$

$$F(t) = 1 - \exp \left[- \left(\frac{t}{\eta} \right)^\beta \right] \quad (3.3)$$

where:

t = time, which is in our case either the flight hours or flight cycles.

β = shape parameter (which has a strong influence on how Weibull graph shape).

η = scale parameter, which is called the characteristic life of a component, that fixes one point of the cumulative distribution function $F(t)$; the “63.2” percentile, which also

mean that the probability failure of an object is 36.78%. This parameter is derived by substituting β for the time t in Equation (3.3) as follows:

$$F(t) = 1 - \exp \left[- \left(\frac{t}{\eta} \right)^\beta \right]$$

$$F(\eta) = 1 - \exp \left[- \left(\frac{\eta}{\eta} \right)^\beta \right] = 1 - \exp (-1) = 0.632 = 63.2\%$$

The function $R(t)$ is normally used when reliabilities are being computed, and the function $F(t)$ is normally used when probabilities are being computed.

3.2 Bathtub Curve

The life of a set of units can be divided into three distinct periods. Figure 3.1 [29] shows the reliability “bathtub curve” which models important instantaneous failure rates vs. time. Following the slope from the start to where it begins to flatten out this can be considered the first period. The first period is characterized by a decreasing failure rate. It is what occurs during the early life of a population of units. This first period is known as an infant mortality period. The next period is the flat segment of the graph. It is called the normal life. Failures occur more in a random sequence during this time. The third period begins at the point where the slope begins to increase and extends to the end of the graph. This is what happens when units become mature and begin to fail at an increasing rate. Bathtub is basically used as a visual model to demonstrate the three main periods of component failure and not adjusted to reflect a graph of the unanticipated behavior for a certain component family [29].

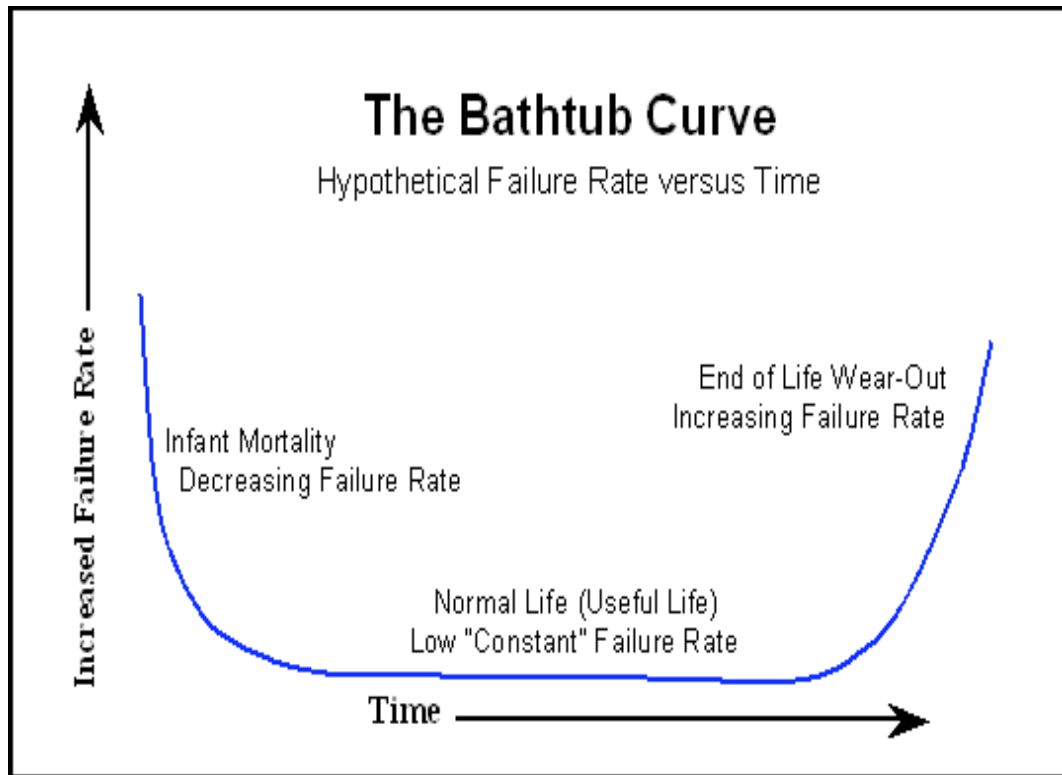


Figure 3.1 The Bathtub Curve

Before fitting the model to the failure data, one needs to define some important statistical characteristics that are widely used in reliability calculations:

Mean Time To Failure (MTTF): Which measures the average time between failures with the modeling assumption that the failed system is not repaired.

Average (median) life ($T_{0.5}$): the life by which half of the units will survive.

$$MTTF = \eta \Gamma \left(1 + \frac{1}{\beta} \right), \text{ where } \Gamma \text{ is the Gamma function} \quad (3.4)$$

$$\Gamma(x) = (x-1) \Gamma(x-1)$$

$$T_{0.5} = \eta (\ln 2)^{\left(\frac{1}{\beta}\right)} \quad (3.5)$$

3.3 Fitting the Weibull Model to the Data

In aviation maintenance, there are usually two units that are used in building maintenance programs, namely the flight hours and flight cycles:

Flight hour (FH): the time from starting up the engine till shut down.

Flight cycle (FC): one take off and one landing.

In this study modeling the failure rate for the bleed air control system will be carried out in terms of both units.

3.3.1 Bleed Air Regulator (BAR-Flight Hour)

To fit the Weibull model, MS EXCEL has the capability to calculate and fit the data on a Weibull plot. Below are the numerical approach steps to fit the model starting with the complementary function as the following:

$$R(t) = \exp \left[- \left(\frac{t}{\eta} \right)^\beta \right]$$

$$F(t) = 1 - R(t)$$

$$F(t) = 1 - \exp \left[- \left(\frac{t}{\eta} \right)^\beta \right]$$

$$F(t) = 1 - \exp\left[-\left(\frac{t}{\eta}\right)^\beta\right]$$

$$\ln[1 - F(t)] = \left[-\left(\frac{t}{\eta}\right)^\beta\right]$$

$$\ln\{\ln[1 - F(t)]\} = \left[-\left(\frac{t}{\eta}\right)^\beta\right]$$

$$\ln\left\{\ln\left[\frac{1}{1 - F(t)}\right]\right\} = \beta \ln(t) - \beta \ln(\eta) \quad (3.6)$$

This equation is a straight line equation

$$y = mx + b$$

where;

$$y = \ln\left\{\ln\left[\frac{1}{1 - F(t)}\right]\right\}, \quad m = \beta, \quad b = -\beta \ln(\eta) \quad ,$$

The two parameters can easily be calculated from the slope of the straight line and the y-intercept point on the graph.

To calculate the reliability, the median rank is best tool to use [32]. Median of a set of data is the number which is in the middle of the data set. To calculate the median, the data should be sorted in ascending order. The median rank formula is:

$$F(t_i) = \frac{i - 0.3}{N + 0.4} \quad 0 \leq i \leq N \quad (3.7)$$

Where I is the failure number and N is the total number of failures.

Table 3-1 shows the main calculations to fit the Weibull model to the failure data using equations (3.1-3.7) for the bleed air regulator (BAR) in term of flight hours (FH).

Table 3-1 Failure analysis for Bleed Air Regulator (FH)

(t) FH	Rank	F(t)	1/(1-F(t))	ln(ln(1/(1-F(t))))	ln(t)
41	1	0.029	1.030	-3.494	3.713
262	2	0.072	1.078	-2.584	5.568
266	3	0.115	1.130	-2.098	5.583
275	4	0.158	1.187	-1.759	5.616
295	5	0.200	1.251	-1.495	5.686
313	6	0.243	1.322	-1.275	5.746
690	7	0.286	1.401	-1.086	6.536
821	8	0.329	1.490	-0.918	6.710
947	9	0.371	1.591	-0.765	6.853
1233	10	0.414	1.708	-0.624	7.117
1315	11	0.457	1.845	-0.492	7.181
1384	12	0.500	2.000	-0.366	7.232
1454	13	0.542	2.186	-0.245	7.282
1565	14	0.585	2.412	-0.127	7.355
1725	15	0.628	2.689	-0.010	7.452
1750	16	0.670	3.038	0.105	7.467
2016	17	0.713	3.492	0.223	7.608
2031	18	0.756	4.105	0.345	7.616
2234	19	0.799	4.978	0.473	7.711
2237	20	0.841	6.324	0.612	7.712
2400	21	0.884	8.666	0.769	7.783
2669	22	0.927	13.764	0.963	7.889
2790	23	0.970	33.428	1.255	7.933

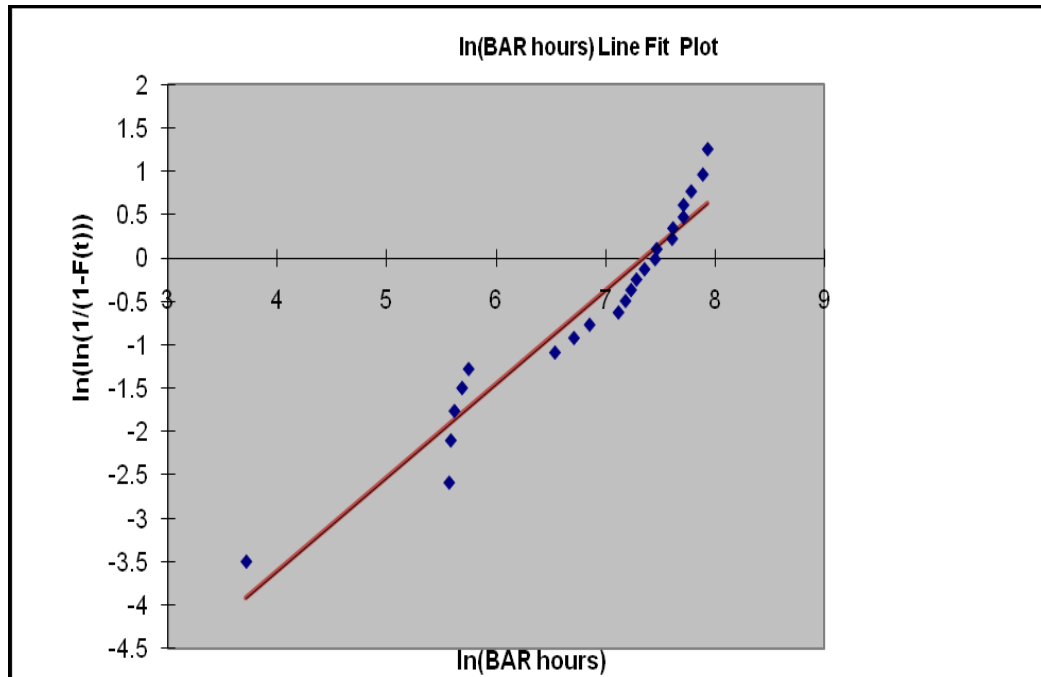


Figure 3.2 Weibull plot for failure data of Bleed Air Regulator (FH)

Using an Excel spread sheet, tables 3-2 and 3-3 show regression analysis output and statistics for the failure data given in table 3-1

Table 3-2 Regression Statistics (BAR-FH)

<i>Regression Statistics</i>	
Multiple R	0.9640915
R Square	0.9294724
Adjusted R Square	0.9261139
Standard Error	0.321034
Observations	23

Table 3-3 Statistics (BAR-FH)

	<i>Coefficients</i>	<i>Standard Error</i>	<i>t Stat</i>	<i>P-value</i>	<i>Lower 95%</i>	<i>Upper 95%</i>	<i>Lower 95.0%</i>	<i>Upper 95.0%</i>
Intercept	-7.9175076	0.448033	-17.6717	4.39E-14	-8.84924	-6.98577	-8.84924	-6.98577
ln(BAR hours)	1.0771718	0.06475	16.63597	1.44E-13	0.942518	1.211826	0.942518	1.211826

Using equation (6), the Weibull parameters are calculated as:

$$\beta = (\text{slope of the line}) = 1.07$$

Since $\beta > 1$ this indicates an increasing failure rate of the bleed air regulator.

$$B = -\beta \ln(\eta) \quad \text{which means that}$$

$$\eta = \exp\left(-\frac{b}{\beta}\right) \exp\left(-\frac{b}{\beta}\right) = \exp\left(-\frac{-7.917}{1.077}\right) = 1557 \text{ (hours)}, \text{ then means 63\% of the}$$

failures occurred up to this time.

Similarly, from equation (4) and (5);

$$\text{MTTF} = 1516 \text{ hours}$$

$$T_{0.5} = 1105 \text{ hours}$$

It is seen that (R Square) is a very important index for the goodness of fit. With an acceptable value of 93%, the goodness of fit is verified. However, if the accuracy of fit is to be enhanced, one could introduce the third Weibull parameter which is called the shift parameter. In this study only two-parameter Weibull model will be used. Three parameter

Weibull model will not improve accuracy significantly, and thus will not affect the final conclusions regarding the developed ANN model.

3.3.2 Goodness-of-Fit Test (BAR-Flight Hour)

The goodness of fit for a statistical model describes how well it fits a set of observations. Measures of goodness of fit typically summarize the discrepancy between observed values and the values expected under the model in question. The test consists of computing a statistic based on the sample of failure times. This statistics is then compared with a critical value obtain from a table of such values [29]. The test compares the distribution function with uniform distribution function of the empirical sample. The idea is to calculate the maximum distance between the theoretical and empirical functions. If this distance exceeds a certain value, which is a fixed value that depends only on the sample size, then the sample does not fit the Weibull method. Kolmogorov-Simirnov (KS) goodness of fit test, which was developed by Lilliefors, is widely used in this practice. The beauty of KS test lies in its flexibility where it can be used with variable of distributions at a small sample [34].

There are several computational methods for the KS. First, sort the data. Then establish the assumed distribution (null hypothesis) and estimate its parameters. Then, obtain both the theoretical (assumed CDF) distribution (F_0) as well as the empirical (F_n) at each data point. Since KS is a distance test, one needs to find the maximum distance $|F_0 - F_n|$ between the theoretical and empirical distributions. Its two basic functions are defined in equation (3.8).

$$F_0(X_i) = P_0(X \leq X_i) \text{ CDF } (X_i); \quad (3.8)$$

$F_0(X_i)$ is the assumed cumulative distribution function evaluated at X_i and $F_n(X_i)$ is the empirical distribution function obtained by the proportion of the data smaller than X_i in the data set size n .

$$F_n(X_i) = i/n; i = 1, \dots, n \quad (3.9)$$

Then, define: $D+ = F_n - F_0$ and $D- = F_0 - F_{n-1}$ for every data point X_i . The KS statistic is:

$$D = \text{Maximum of all } D+ \text{ and } D- (\geq 0); \text{ for } i = 1, \dots, n \quad (3.10)$$

The KS logic is as follows: if the maximum departure between the assumed CDF and empirical distributions is small, then the assumed CDF will likely be correct. But if this discrepancy is "large" then the assumed F_0 is likely not the underlying data distribution.

Using equations (3.8), (3.9) and (3.10)

Table 3-4 shows calculation for KS test with the following sample of calculations for Row 1 in table 3.1:

$$F_0 = F(t) = 1 - \exp \left[- \left(\frac{t}{\eta} \right)^\beta \right] = 1 - \exp \left[- \left(\frac{41}{1556} \right)^{1.077} \right] = 0.01971$$

$$F_{n-1}(1) = (1-1)/23 = 0 \quad D+ = F_n - F_0 = 0.043 - 0.019 = 0.023$$

Table 3-4 KS GOF test for Bleed Air Regulator (FH)

ROW	FH	Fo	Fn	Fn-1	D+	D-
1	41	0.019718	0.043478	0	0.023761	0.019718
2	262	0.13653	0.086957	0.043478	-0.04957	0.093052
3	266	0.138613	0.130435	0.086957	-0.00818	0.051657
4	275	0.14329	0.173913	0.130435	0.030623	0.012855
5	295	0.153634	0.217391	0.173913	0.063758	-0.02028
6	313	0.162882	0.26087	0.217391	0.097988	-0.05451
7	690	0.340669	0.304348	0.26087	-0.03632	0.0798
8	821	0.394856	0.347826	0.304348	-0.04703	0.090508
9	947	0.443329	0.391304	0.347826	-0.05202	0.095502
10	1233	0.540835	0.434783	0.391304	-0.10605	0.149531
11	1315	0.565794	0.478261	0.434783	-0.08753	0.131011
12	1384	0.585828	0.521739	0.478261	-0.06409	0.107567
13	1454	0.605281	0.565217	0.521739	-0.04006	0.083542
14	1565	0.634406	0.608696	0.565217	-0.02571	0.069188
15	1725	0.672887	0.652174	0.608696	-0.02071	0.064191
16	1750	0.678546	0.695652	0.652174	0.017106	0.026372
17	2016	0.733326	0.73913	0.695652	0.005805	0.037674
18	2031	0.736136	0.782609	0.73913	0.046473	-0.00299
19	2234	0.771514	0.826087	0.782609	0.054573	-0.0111
20	2237	0.772001	0.869565	0.826087	0.097564	-0.05409
21	2400	0.797041	0.913043	0.869565	0.116002	-0.07252
22	2669	0.832716	0.956522	0.913043	0.123805	-0.08033
23	2790	0.846725	1	0.956522	0.153275	-0.1098
				MAX=	0.153275	0.149531

From the table above,

$$\text{Max } D^+ = 0.153$$

$$\text{Max } D^- = 0.149$$

Sample size = 23,

The critical value (CV) for KS test can be calculated using (3.11):

$$CV = \frac{1.36}{\sqrt{n}} \quad \text{where } (n) \text{ is the sample size} \quad (3.11)$$

$$CV = 0.28$$

Since $\text{max } D^+ = 0.153 < CV = 0.280 \Rightarrow$ The sample is accepted.

3.3.3 Weibull Analysis for Bleed Air Regulator (Flight Cycles)

Following the same procedures for the flight hours, the following tables and calculations demonstrate the Weibull analysis for the BAR in terms of flight cycles (FC). Table **3-5** shows the failure history for the BAR with the required calculation for fitting the data to the Weibull model.

Table 3-5 BAR Weibull failure analysis (FC)

(FC)	Rank	F(t)	1/(1-F(t))	ln(ln(1/(1-F(t))))	ln(FC)	CDF
76	1	0.030	1.031	-3.494	4.331	0.022
345	2	0.073	1.078	-2.585	5.844	0.113
394	3	0.115	1.130	-2.099	5.976	0.130
396	4	0.158	1.188	-1.760	5.981	0.131
462	5	0.201	1.251	-1.495	6.136	0.153
517	6	0.244	1.322	-1.276	6.248	0.172
1104	7	0.286	1.401	-1.087	7.007	0.355
1215	8	0.329	1.490	-0.919	7.102	0.386
1461	9	0.372	1.592	-0.766	7.287	0.450
1897	10	0.415	1.708	-0.625	7.548	0.550
2001	11	0.457	1.843	-0.492	7.601	0.572
2053	12	0.500	2.000	-0.367	7.627	0.582
2209	13	0.543	2.187	-0.245	7.700	0.612
2329	14	0.585	2.412	-0.127	7.753	0.633
2395	15	0.628	2.690	-0.011	7.781	0.645
2512	16	0.671	3.039	0.106	7.829	0.664
2981	17	0.714	3.493	0.224	8.000	0.733
2984	18	0.756	4.105	0.345	8.001	0.733
3271	19	0.799	4.979	0.473	8.093	0.768
3495	20	0.842	6.324	0.612	8.159	0.793
3739	21	0.885	8.667	0.770	8.227	0.817
4097	22	0.927	13.765	0.964	8.318	0.847
4322	23	0.970	33.429	1.255	8.371	0.864

Table 3-6 and Table 3-7 represents the Regression analysis and statistics for data given in Table 3-5

Table 3-6 Regression Statistics (BAR-FC)

<i>Regression Statistics</i>	
Multiple R	0.97211
R Square	0.944999
Adjusted R Square	0.94238
Standard Error	0.283503
Observations	23

Table 3-7 Statistics (BAR-FC)

	<i>Coefficients</i>	<i>Standard Error</i>	<i>t Stat</i>	<i>P-value</i>	<i>Lower 95%</i>	<i>Upper 95%</i>	<i>Lower 95.0%</i>	<i>Upper 95.0%</i>
Intercept	-8.60946	0.428512	-20.0915	3.42E-15	-9.5006	-7.71832	-9.5006	-7.71832
ln(FC)	1.110828	0.05848	18.99498	1.05E-14	0.989212	1.232444	0.989212	1.232444

From regression output, it is clear that data shows a strong fit based on the value of (R Square) which is almost 95%. In order to estimate the Weibull parameters for this model, the same procedures used in the flight hour's calculations will be implemented.

Using equation (3.6), we can calculate the Weibull parameters as:

$$\beta = (\text{slope of the line}) = 1.11$$

Since $\beta > 1$ this indicates an increasing failure rate of the bleed air regulator.

$$B = -\beta \ln(\eta) \quad \text{which means that}$$

$$\eta = \exp - \left(\frac{b}{\beta} \right) \exp - \left(\frac{b}{\beta} \right) = \exp - \left(\frac{-8.609}{1.110} \right) = 1806 \text{ (cycles)}, \text{ than means } 63\% \text{ of the}$$

failures occurred up to this time.

Similarly, from Equations (3.4) and (3.5);

$$\text{MTTF} = 1738 \text{ cycles}$$

$$T_{0.5} = 1202 \text{ cycles}$$

3.3.4 Weibull Analysis for High Stage Valve (Flight Hours)

Same procedures will be followed for analysis for this valve just like the bleed air regulator. First, the Weibull analysis will be performed in terms of flight hours and cycles followed by the goodness of fit test.

Table 3-8 shows the failure analysis for the high stage valve in terms of flight hours with the necessary calculations to estimate the Weibull parameters. The main difference between the high stage valve and the bleed air regulator data is the number of observations or failures. For the high stage valve, the number of failures are less than the BAR. This gives a good indication about how our analysis would be affected as the number of observations is decreasing. Following the same steps that were used in the BAR calculations, Figure 3.3 shows the Weibull plot for high stage valve.

Table 3-8 Failure analysis for High Stage Valve (Flight Hour)

t (FH)	Rank	F(t)	1/(1-F(t))	ln(ln(1/(1-F(t))))	ln(t)
234	1	0.049	1.051	-2.999	5.455
236	2	0.118	1.134	-2.074	5.464
500	3	0.188	1.231	-1.572	6.215
760	4	0.257	1.346	-1.214	6.633
989	5	0.326	1.485	-0.929	6.897
1022	6	0.396	1.655	-0.685	6.930
1211	7	0.465	1.870	-0.468	7.099
1641	8	0.535	2.149	-0.268	7.403
1786	9	0.604	2.526	-0.076	7.488
1901	10	0.674	3.064	0.113	7.550
1923	11	0.743	3.892	0.307	7.562
2100	12	0.813	5.333	0.515	7.650
2155	13	0.882	8.471	0.759	7.676
2712	14	0.951	20.571	1.107	7.905

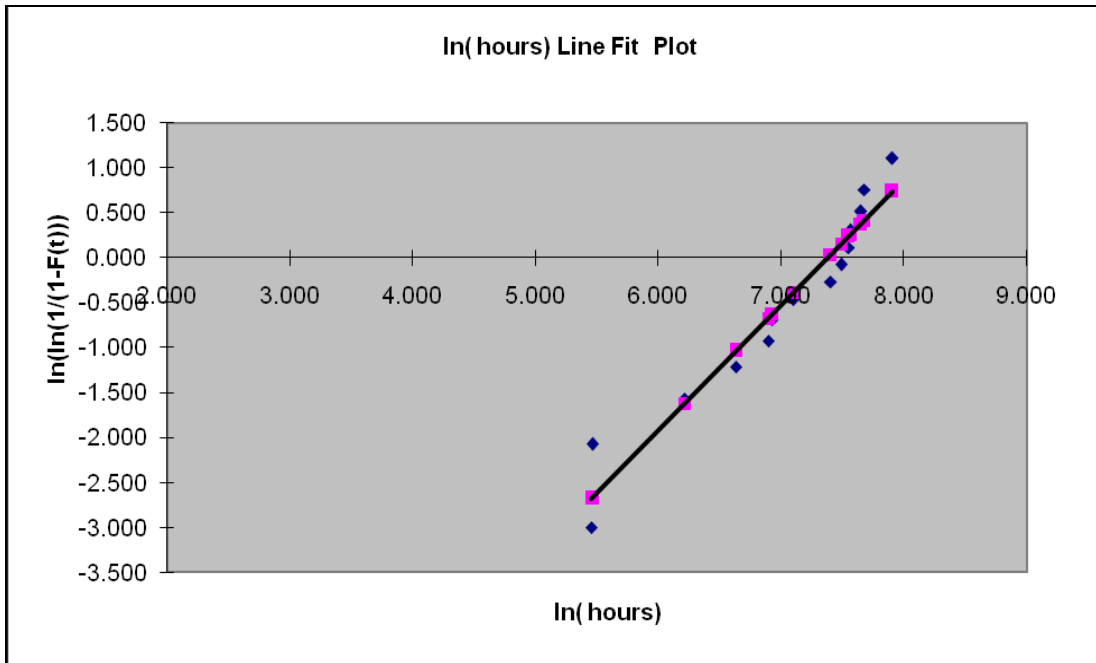


Figure 3.3 Weibull plot for high stage valve (FH)

Similarly, using an Excel spread sheet, below are the regression analysis for the high stage bleed valve. Table 3-9 represents regression analysis for data given in Table 3-8

Table 3-9 Regression Statistics (HSV-FH)

<i>Regression Statistics</i>	
Multiple R	0.970156
R Square	0.941203
Adjusted R Square	0.936304
Standard Error	0.288974
Observations	14

The results show that R square value is almost (94%) which shows a strong index of fit. Although the sample data for the high stage valve is less than those for the bleed air regulator, this fact did not affect the index of fit for the data which shows the power of the Weibull method for our analysis with limited number of observations. Another regression output in Table 3-10 represents another statistics for data give in Table 3-8.

Table 3-10 Statistics (HSV-FH)

	<i>Coefficients</i>	<i>Standard Error</i>	<i>t Stat</i>	<i>P-value</i>	<i>Lower 95%</i>	<i>Upper 95%</i>	<i>Lower 95.0%</i>	<i>Upper 95.0%</i>
Intercept	-10.2946	0.7084	-14.5319	0.0000	-11.8381	-8.7511	-11.8381	-8.7511
ln(BAR hours)	1.3953	0.1007	13.8598	0.0000	1.1760	1.6147	1.1760	1.6147

Using equation (3.6), Weibull parameters are:

$$\beta = (\text{slope of the line}) = 1.39$$

Since $\beta > 1$ this indicates an increasing failure rate of the high stage valve.

$$B = -\beta \ln(\eta) \quad \text{which means that}$$

$$\eta = \exp\left(-\frac{b}{\beta}\right) \exp\left(-\frac{b}{\beta}\right) = \exp\left(-\left(\frac{-10.294}{1.395}\right)\right) = 1600 \text{ (hours)}, \text{ than means 63\% of the}$$

failures occurred up to this time.

Similarly, from Equations (3.4) and (3.5);

$$\text{MTTF} = 1459 \text{ hours}$$

$$T_{0.5} = 1229 \text{ hours}$$

3.3.5 Goodness-of-Fit Test (High Stage Valve-Flight Hour)

Similar to the BAR, the goodness of fit for the data for high stage valve will be checked. Since the number of data is relatively smaller, this check will indicate any effect of the size on the fitting the model into the Weibull model. Following the same calculations that were performed for the BAR,

Table 3-11 shows the KS goodness of fit test calculations.

From the

Table 3-11,

Max D^+ = 0.149

Max D^- = 0.145

Sample size = 14,

The critical value CV for KS test for data of size 14 = 0.360

Since **max D^+ = 0.149 < CV = 0.360** \Rightarrow the sample is accepted.

Table 3-11 KS GOF test for High Stage Valve (FH)

Rank	FH	Fo	Fn	Fn-1	D+	D-
1	234	0.067	0.071	0.000	0.005	0.067
2	236	0.068	0.143	0.071	0.075	-0.004
3	500	0.180	0.214	0.143	0.034	0.037
4	760	0.299	0.286	0.214	-0.013	0.085
5	989	0.401	0.357	0.286	-0.044	0.115
6	1022	0.415	0.429	0.357	0.014	0.058
7	1211	0.493	0.500	0.429	0.007	0.064
8	1641	0.645	0.571	0.500	-0.074	0.145
9	1786	0.688	0.643	0.571	-0.045	0.117
10	1901	0.719	0.714	0.643	-0.005	0.076
11	1923	0.725	0.786	0.714	0.061	0.011
12	2100	0.768	0.857	0.786	0.090	-0.018
13	2155	0.780	0.929	0.857	0.149	-0.077
14	2712	0.875	1.000	0.929	0.125	-0.053
				MAX=	0.149	0.145

3.3.6 Weibull Analysis for High Stage Valve (Flight Cycles)

Due to the fact that high stage valve works under extreme conditions in terms of pressure and temperature, it is imperative to take a look at the data from different angle, and this time from cycles point of view. Engines are pushed to the limit during the takeoff phase of the flight. At this phase, all engine systems, especially bleed air system, are exposed to a tremendous amount of power that would make any malfunction leads to a catastrophic subsequence. Table **3-12** shows the failure data for the high stage valve in terms of flight cycles (FC), with the necessary calculations to estimate the Weibull parameters.

Table 3-12 High stage valve failure data (FC)

t(FC)	Rank	F(t)	1/(1-F(t))	ln(ln(1/(1-F(t))))	ln(t)	CDF
337	1	0.049	1.051	-2.999	5.820	0.064
346	2	0.118	1.134	-2.074	5.846	0.066
930	3	0.188	1.231	-1.572	6.835	0.226
1014	4	0.257	1.346	-1.214	6.922	0.250
1510	5	0.326	1.485	-0.929	7.320	0.388
1655	6	0.396	1.655	-0.685	7.412	0.426
1890	7	0.465	1.870	-0.468	7.544	0.484
2707	8	0.535	2.149	-0.268	7.904	0.657
2806	9	0.604	2.526	-0.076	7.940	0.675
3235	10	0.674	3.064	0.113	8.082	0.743
3238	11	0.743	3.892	0.307	8.083	0.744
3311	12	0.813	5.333	0.515	8.105	0.754
3744	13	0.882	8.471	0.759	8.228	0.809
4000	14	0.951	20.571	1.107	8.294	0.836

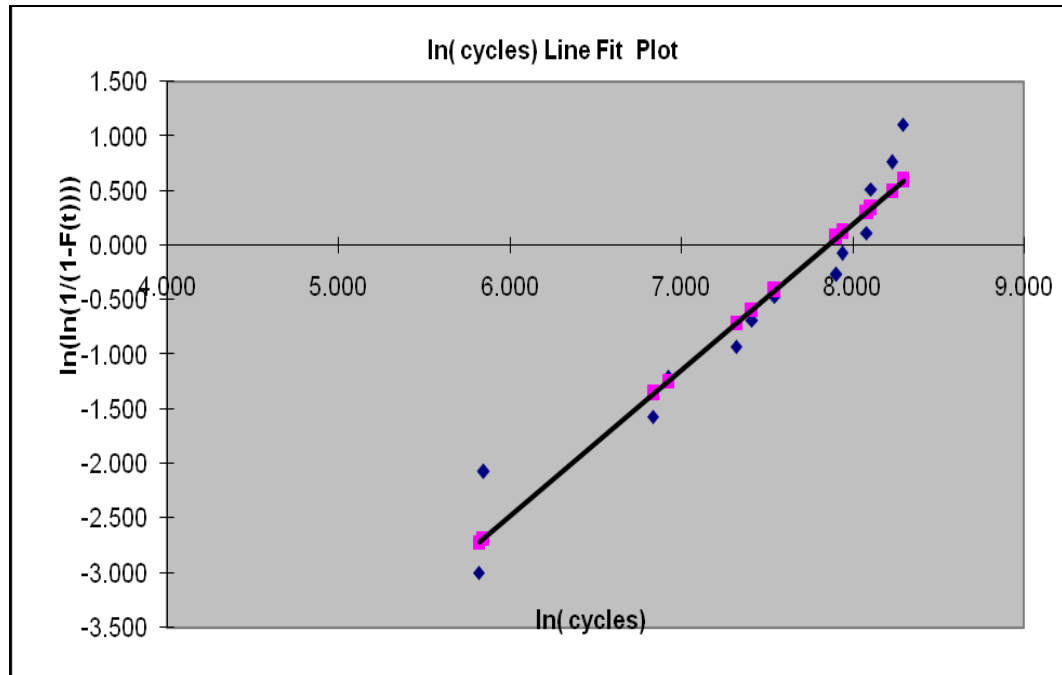


Figure 3.4 Weibull plot for high stage valve (FC)

Regression and statistical data for the high stage valve are given in Table 3-13 and Table 3-14.

Table 3-13 Regression Statistics (HSV-FC)

<i>Regression Statistics</i>	
Multiple R	0.96703199
R Square	0.93515088
Adjusted R Square	0.92974679
Standard Error	0.3034834
Observations	14

Table 3-14 Statistics (HSV-FC)

	<i>Coefficients</i>	<i>Standard Error</i>	<i>t Stat</i>	<i>P-value</i>	<i>Lower 95%</i>	<i>Upper 95%</i>	<i>Lower 95.0%</i>	<i>Upper 95.0%</i>
Intercept	-10.505258	0.762281	-13.7814	1.02E-08	-12.1661	-8.84439	-12.1661	-8.84439
ln (cycles)	1.33790498	0.101706	13.15465	1.73E-08	1.116307	1.559503	1.116307	1.559503

Using Equation (3.6), Weibull parameters are:

$$\beta = (\text{slope of the line}) = 1.338$$

Since $\beta > 1$ this indicates an increasing failure rate of the high stage valve.

$$B = -\beta \ln(\eta) \quad \text{which means that}$$

$$\eta = \exp\left(-\frac{b}{\beta}\right) \exp\left(-\frac{b}{\beta}\right) = \exp\left(-\frac{-10.505}{1.338}\right) = 2570 \text{ (cycles)}, \text{ than means 63\% of the}$$

failures occurred up to this time.

Similarly, from Equations (3.4) and (3.5);

$$\text{MTTF} = 2359 \text{ cycles}$$

$$T_{0.5} = 1954 \text{ cycles}$$

3.3.7 Goodness-of-Fit Test (High Stage Valve -Flight Cycle)

Table 3-15 shows KS goodness of fit calculations for the high stage valve (cycles).

Table 3-15 KS test for high stage valve (FC)

Rank	Cycles	Fo	Fn	Fn-1	D+	D-
1	337	0.064	0.071	0.000	0.007	0.064
2	346	0.066	0.143	0.071	0.077	-0.005
3	930	0.227	0.214	0.143	-0.012	0.084
4	1014	0.251	0.286	0.214	0.035	0.036
5	1510	0.388	0.357	0.286	-0.031	0.102
6	1655	0.426	0.429	0.357	0.003	0.069
7	1890	0.485	0.500	0.429	0.015	0.056
8	2707	0.658	0.571	0.500	-0.086	0.158
9	2806	0.675	0.643	0.571	-0.032	0.104
10	3235	0.743	0.714	0.643	-0.029	0.101
11	3238	0.744	0.786	0.714	0.042	0.030
12	3311	0.754	0.857	0.786	0.103	-0.032
13	3744	0.809	0.929	0.857	0.120	-0.048
14	4000	0.836	1.000	0.929	0.164	-0.093
				MAX=	0.164	0.158

From the table above,

Max D^+ = 0.164

Max D^- = 0.158

Sample size = 14,

From appendix, the critical value CV for KS test for data of size 14 = 0.360

Since max D^+ = 0.149 < CV = 0.360 \Rightarrow the sample is accepted.

3.3.8 Weibull Analysis Pressure Regulator and Shutoff Valve (Flight Hours)

Following the same methodology used for bleed air regulator and high stage valve, estimating of Weibull parameters will be conducted for the data in terms of flight hours (FH) and flight cycles (FC). Among the three valves that are studied in this work, the PRSOV got the least number of failure data gathered from the aircraft logbook. The following calculations will reveal how significant the simulation process is affected by drastically reducing the number of analyzed data.

Table **3-16** shows the failure analysis for the high stage valve in terms of flight hours (FH) with the necessary calculations to estimate the Weibull parameters.

Table 3-16 PRSOV failure data (Flight Hour)

t (FH)	Rank	F(t)	1/(1-F(t))	ln(ln(1/(1-F(t))))	ln(t)	CDF
77	1	0.061	1.065	-2.759	4.344	0.038
427	2	0.149	1.175	-1.823	6.057	0.236
512	3	0.237	1.310	-1.308	6.238	0.282
954	4	0.325	1.481	-0.935	6.861	0.488
1036	5	0.412	1.701	-0.632	6.943	0.521
1117	6	0.500	2.000	-0.367	7.018	0.551
1256	7	0.588	2.426	-0.121	7.136	0.599
1340	8	0.675	3.081	0.118	7.200	0.626
1360	9	0.763	4.222	0.365	7.215	0.633
1990	10	0.851	6.706	0.643	7.596	0.786
2064	11	0.939	16.286	1.026	7.632	0.799

Following the same approach for estimating the Weibull parameters, Figure 3.5 shows the Weibull plot for the PRSOV in terms of (FH).

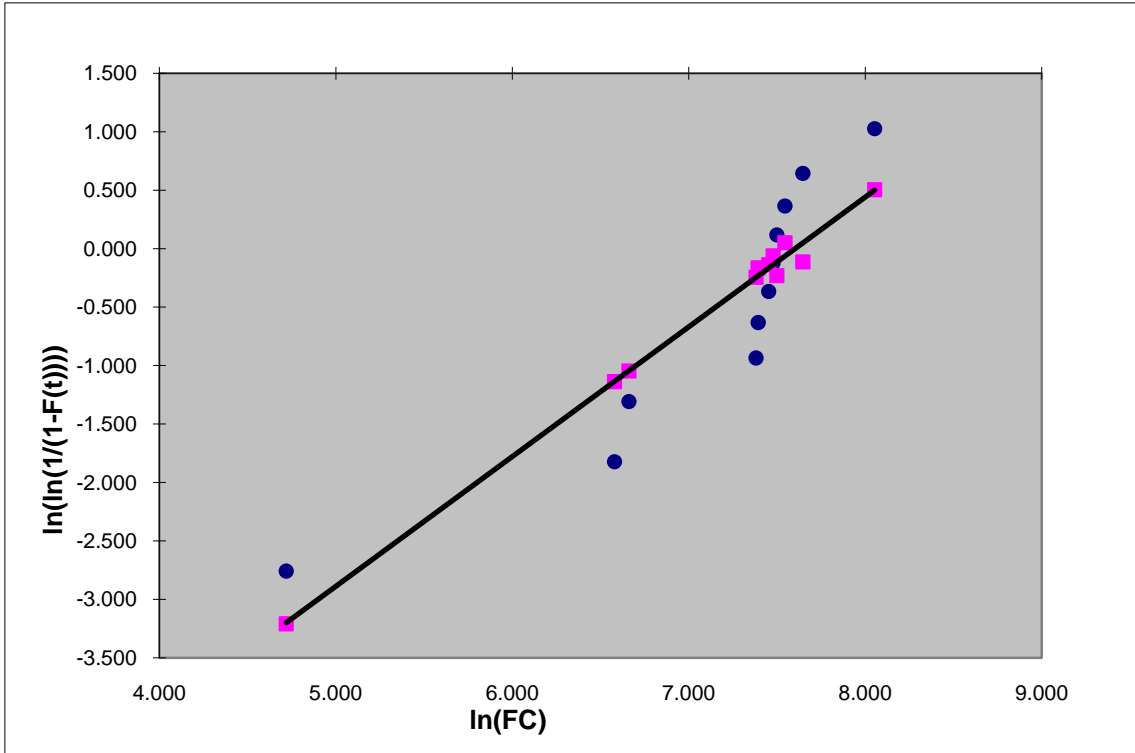


Figure 3.5 PRSOV Weibull plot (FH)

From above graph, regression and statistical analysis for this valve are represented in Table 3-17 and Table 3-18

Table 3-17 Regression Statistics (PRSOV-FH)

<i>Regression Statistics</i>	
Multiple R	0.940446
R Square	0.884439
Adjusted R Square	0.871599
Standard Error	0.402766
Observations	11

From above table it can be noticed that R Square is approximately (88%) which shows a weak index of fit. This clearly indicates how Weibull fit accuracy was affected by the number of data in this case. The index of fit for PRSOV model is least value compared to the other valves. The goodness of fit test will be conducted again to ensure and validate the Weibull model for this particular valve.

Regression analysis was similarly utilized to estimate the Weibull parameters for PRSOV as following.

Table 3-18 Statistics (PRSOV-FH)

	<i>Coefficients</i>	<i>Standard Error</i>	<i>t Stat</i>	<i>P-value</i>	<i>Lower 95%</i>	<i>Upper 95%</i>	<i>Lower 95.0%</i>	<i>Upper 95.0%</i>
Intercept	-8.1684	0.9287	-8.7952	0.0000	-10.2693	-6.0675	-10.2693	-6.0675
ln(PRSOV (FH))	1.1323	0.1364	8.2994	0.0000	0.8236	1.4409	0.8236	1.4409

Using equation (3.6), Weibull parameters can be estimated as the following:

$$\beta = (\text{slope of the line}) = 1.132$$

Since $\beta > 1$ this indicates an increasing failure rate of the pressure regulator shut off valve

$\eta = \exp\left(-\frac{b}{\beta}\right) \exp\left(-\frac{b}{\beta}\right) = \exp\left(-\frac{-8.168}{1.132}\right) = 1360$ (hours), than means 63% of the failures occurred up to this time.

Similarly, from equation (3.4) and (3.5);

MTTF = 1300 hours

$T_{0.5}$ = 983 hours

3.3.9 Goodness-of-Fit Test (PRSOV-Flight Hours)

Similar to previous analysis conducted for all valves, **Kolmogorov-Smirnov** will indicate whether Weibull distribution is valid to the PRSOV analysis. Since Weibull did not show a strong fit to the model, this test validates whether the analysis is accepted or not. Table 3-19 shows KS GOF test for PRSOV in terms of flight hours (FH):

Table 3-19 KS GOF test for PRSOV (FH)

ROW	FH	Fo	Fn	Fn-1	D+	D-
1	77	0.038	0.091	0.000	0.053	0.038
2	427	0.236	0.182	0.091	-0.055	0.146
3	512	0.282	0.273	0.182	-0.009	0.100
4	954	0.489	0.364	0.273	-0.125	0.216
5	1036	0.521	0.455	0.364	-0.066	0.157
6	1117	0.551	0.545	0.455	-0.006	0.097
7	1256	0.600	0.636	0.545	0.037	0.054
8	1340	0.627	0.727	0.636	0.101	-0.010
9	1360	0.633	0.818	0.727	0.185	-0.095
10	1990	0.786	0.909	0.818	0.123	-0.032
11	2064	0.799	1.000	0.909	0.201	-0.110
MAX=					0.201	0.216

From the table above,

$$\text{Max } D^+ = 0.201$$

$$\text{Max } D^- = 0.216$$

Sample size (n) = 11,

$$\text{The critical value (CV) } = \frac{1.36}{\sqrt{n}} = 0.410$$

Since $\text{max } D^+ = 0.216 < \text{CV} = 0.410 \Rightarrow$ the sample is accepted.

3.3.10 Weibull Analysis for Pressure Regulator and Shutoff Valve (Flight Cycles)

As mentioned earlier, the simulation process is performed from different perspective which is the flight cycles. Such an approach will make this study comprehensive in terms of maintenance planning strategy. Following the same procedures for modeling the failure rate of the bleed air following the same procedures for modeling the failure rate of the bleed air system components, below are the calculations and output for the PRSOV for Weibull method.

Table 3-20 PRSOV failure data (FC)

t (FC)	Rank	F(t)	1/(1-F(t))	ln(ln(1/(1-F(t))))	ln(t)	CDF
112	1	0.061	1.065	-2.759	4.718	0.040
720	2	0.149	1.175	-1.823	6.579	0.274
781	3	0.237	1.310	-1.308	6.661	0.296
1605	4	0.325	1.481	-0.935	7.381	0.543
1625	5	0.412	1.701	-0.632	7.393	0.548
1725	6	0.500	2.000	-0.367	7.453	0.572
1769	7	0.588	2.426	-0.121	7.478	0.582
1806	8	0.675	3.081	0.118	7.499	0.590
1891	9	0.763	4.222	0.365	7.545	0.609
2093	10	0.851	6.706	0.643	7.646	0.651
3145	11	0.939	16.286	1.026	8.054	0.809

Figure 3.6 shows Weibull plot for the above table.

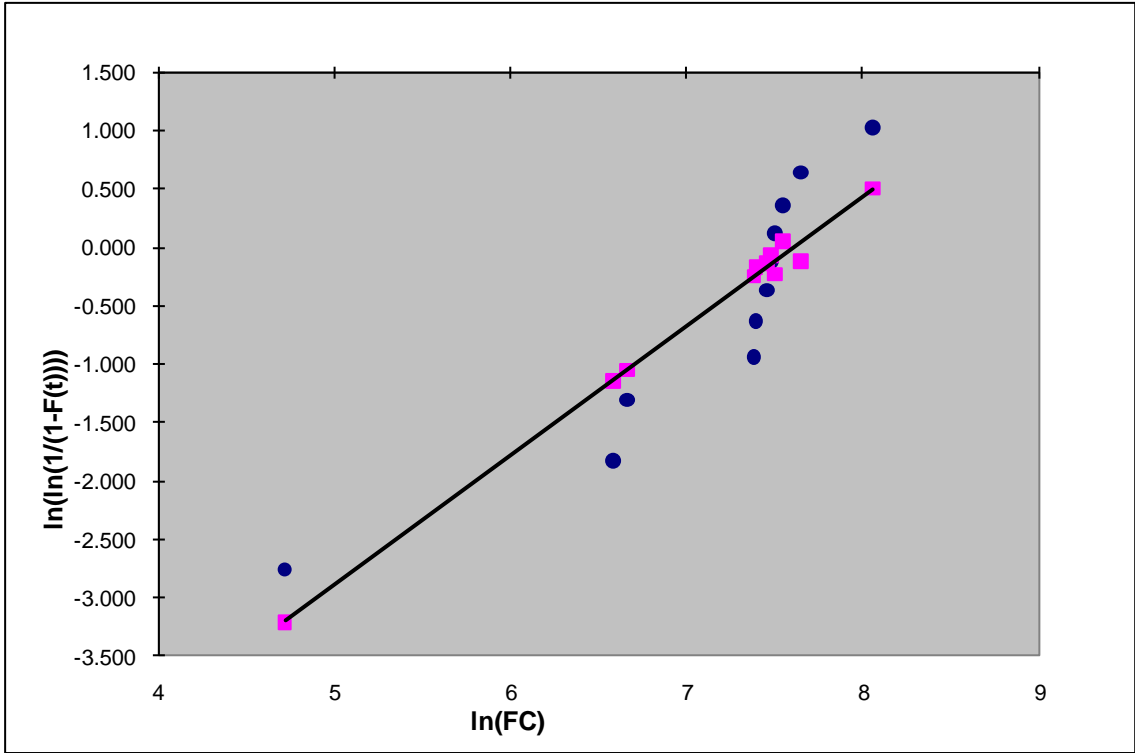


Figure 3.6 PRSOV Weibull Plot (FC)

Table 3-21 and Table 3-22 show the regression output and statistics for the above figure:

Table 3-21 Regression Statistics (PRSOV-FC)

<i>Regression Statistics</i>	
Multiple R	0.893
R Square	0.797
Adjusted R Square	0.775
Standard Error	0.533
Observations	11

The above graph shows a poor fit which indicated by a (R Square = 0.797). Since the PRSOV got the least amount of data, it is clear that Weibull method does not give a good and accurate simulation output for such a size of data. Although Weibull model has an advantage of being accurate with limited number of data, this feature apparently got drastically affected with this sample size at the above table. The goodness of fit test is demonstrated to ensure whether Weibull model is accepted for this sample or not.

Below are the regression outputs for the PRSOV (FC) model.

Table 3-22 Statistics (PRSOV-FC)

	<i>Coefficients</i>	<i>Standard Error</i>	<i>t Stat</i>	<i>P-value</i>	<i>Lower 95%</i>	<i>Upper 95%</i>	<i>Lower 95.0%</i>	<i>Upper 95.0%</i>
Intercept	-8.463908017	1.34325	-6.30106	0.000141	-11.5026	-5.42526	-11.5026	-5.42526
ln(FC)	1.113545932	0.187094	5.951806	0.000215	0.69031	1.536781	0.69031	1.536781

Using Equation (3.6), Weibull parameters can be estimated as the following.

$$\beta = (\text{slope of the line}) = 1.11$$

Since $\beta > 1$ this indicates an increasing failure rate of the pressure regulator shut off valve

$$B = -\beta \ln(\eta) \quad \text{which means that}$$

$$\eta = \exp\left(-\frac{b}{\beta}\right) \exp\left(-\frac{b}{\beta}\right) = \exp\left(-\frac{-8.463}{1.113}\right) = 2005 \text{ (cycles)}, \text{ than means 63\% of the failures}$$

occurred up to this time.

Similarly, from Equations (3.4) and (3.5);

MTTF = 1926 cycles

$T_{0.5}$ = 1442 cycles

3.3.11 Goodness of Fit Test (PRSOV-Flight Cycles)

Similar to flight hours (FH) approach,

Table 3-23 shows the GOF test for the PRSOV in terms of flight cycles (FC).

Table 3-23 KS GOF test for PRSOV (FC)

ROW	FC	Fo	Fn	Fn-1	D+	D-
1	112	0.040	0.091	0.000	0.051	0.040
2	720	0.274	0.182	0.091	-0.092	0.183
3	781	0.296	0.273	0.182	-0.023	0.114
4	1605	0.543	0.364	0.273	-0.179	0.270
5	1725	0.572	0.455	0.364	-0.117	0.208
6	1769	0.582	0.545	0.455	-0.037	0.127
7	1891	0.609	0.636	0.545	0.027	0.064
8	1625	0.548	0.727	0.636	0.179	-0.089
9	2093	0.651	0.818	0.727	0.167	-0.077
10	1806	0.590	0.909	0.818	0.319	-0.228
11	3145	0.809	1.000	0.909	0.191	-0.100
				MAX=	0.319	0.270

From

Table 3-23,

Max D+ = 0.201

Max D- = 0.216

Sample size (n) = 11,

The critical value (CV) = $\frac{1.36}{\sqrt{n}}$ = 0.410

Since max D+ = 0.319 < CV = 0.410 \Rightarrow the sample is accepted.

Chapter 4

ANN METHODOLOGY

4.1 Artificial Neural Network

4.1.1 Introduction

Artificial Neural Network is an information processing system that has a certain performance characteristics in common with biological neural network [28]. It's a non-linear structure based on the function of human brain, which is a powerful tool for modeling, especially when underlying data relationship is unknown. ANN can identify and learn correlated patterns between input data and corresponding target values. ANN is composed of interconnected neurons that are arranged in systematic structure to perform a task using the concept of artificial intelligence. ANNs have become the focus of much attention because of their wide range of applicability and the ease with which they can treat complicated problems. What makes ANN unique are their adaptive nature, where “learning by example” replaces “programming” in solving problems. They have the ability to learn from experience in order to improve their performance and to adapt themselves to changes in the environment.

In addition to that they are able to deal with incomplete information or data and can be very effective especially in situations where it is not possible to define the rules or steps that lead to the solution of a problem. ANN's have been used for a wide variety of

applications where statistical methods are traditionally implemented. The problems which were normally solved through classical statistical methods, such as multiple regressions, are being tackled by ANN's.

4.1.2 Artificial Neural Networks Classifications

ANNs can be categorized based on many aspects. They can be classified according to the following attributions.

Applications

- Classification
- Clustering
- Function approximation
- Prediction

Connection Type

- Static (feed forward)
- Dynamic (feedback)

Topology

- Single layer
- Multilayer
- Recurrent
- Self-organized

Learning Methods

- Supervised
- Unsupervised

In this study, the most popular algorithm which is the back-propagation algorithm is utilized to train the network. The back-propagation (BP) artificial neural network (ANN) is a well-known and widely applied mathematical model for prediction applications. The back propagation ANN algorithm concept is based on a gradient descent algorithm that is used to continually adjust the network weights to maximize performance, using some criterion function. The aim of the network is to train the network to achieve a balance between the ability to respond correctly to the input patterns that are used for training and the ability to provide a good responses to the input that are similar.

BP process could be divided into two segments, which are the forward-propagation and the back-propagation. The first segment simply starts by sending input signals thorough the nodes of each layer in the network. The back-propagation segment calculates the error by referring to the stopping criteria that was set for the network. Commonly, neural networks are adjusted, or trained, so that a particular input leads to a specific target output. Figure 4.1 shows a simple perceptron and could it is processed and Figure 4.2 shows the basic concept of the back-propagation algorithm. The network is adjusted, based on a comparison of the output and the target, until the network output matches the desired target. The stopping criteria is basically a preset value for the difference between the output and the desired output of the network, in most of the

literatures, this difference is referred to as the error function or the mean square error (MSE).

Transforming the input signals into output signals is accomplished by an activation function which could be a sigmoid- function or any other function depends on the structure and the nature of the network. Sigmoid function is utilized which is the most suitable function to serve the purpose of our problem..

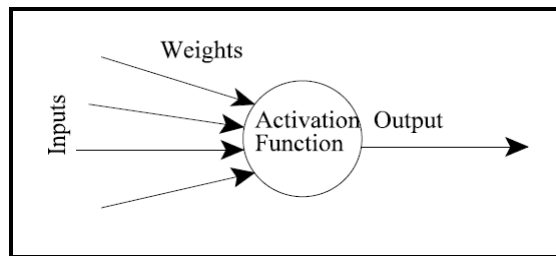


Figure 4.1 Simple Perceptron

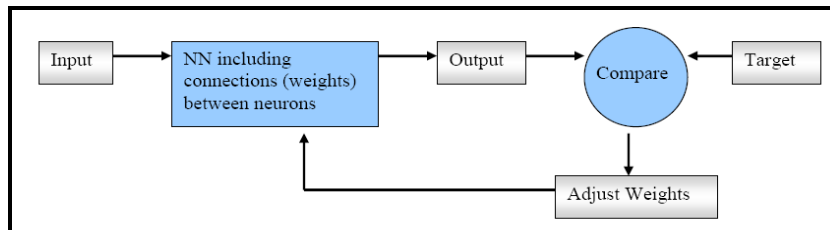


Figure 4.2 Working Flow Chart for the BP ANN process

The basic mathematical model of the back-propagation algorithm [33] is described as follows:

$$x_j = \text{normalized } X_d \quad 1 < d \leq M$$

(4.1)

$$\text{net}_k = \sum_{j=1}^{k-1} W_{kj} x_j \quad m \leq k \leq N + n \quad (4.2)$$

$$x_k = f(\text{net}_k) \quad m < k \leq N + n \quad (4.3)$$

$$O_s = X_{N+s} \quad 1 \leq s \leq n \quad (4.4)$$

$$f(\text{net}) = \frac{1}{1 + e^{-\text{net}}} \quad (4.5)$$

Where m is the number of inputs to the network, n is the number of outputs of the ANN, and X_d represents the actual inputs to the ANN (which have to be normalized and then initially stored in x_j). The non-linear activation function $f(\text{net}_k)$ in equation (4.5) is log-sigmoid function and it depends on the desired output data range. N is a constant, which represents the number of intermediate neurons in the ANN. It can be any integer as long as it is not less than m . The value of $N+m$ determines how many neurons are there in the network (if the inputs are included as neuron). W is the weight matrix in each layer whose size depends on the number of neurons in the corresponding adjacent layers of ANN. W_{kj} are the elements of the weight matrix. The term x_k is called the “activation level” of the neuron, and O_s is the output from ANN.

Figure 4.3 and Figure 4.4 illustrate the multiple ANN configurations and structures used in our analysis.

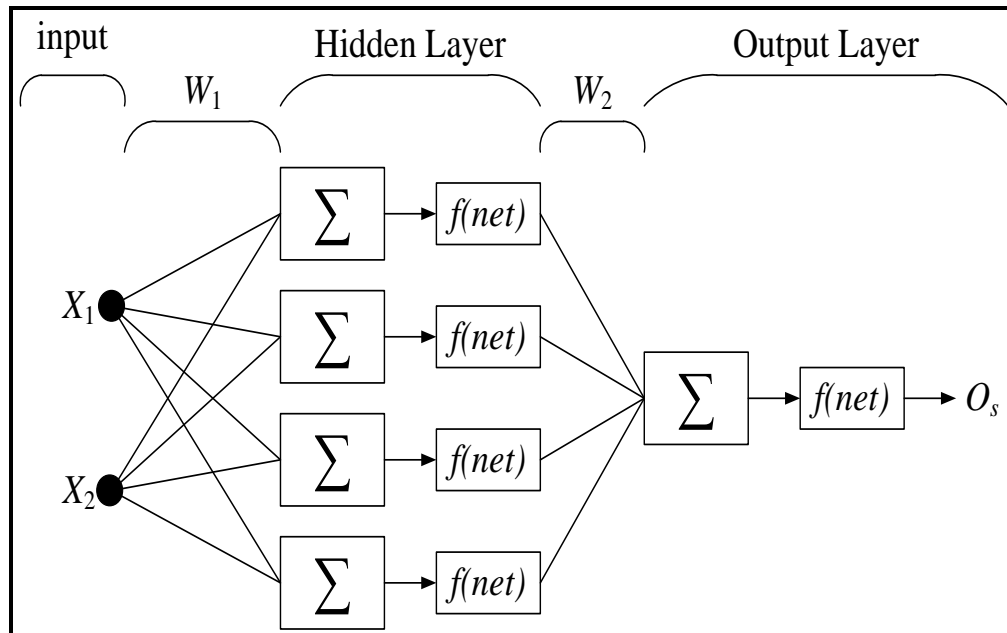


Figure 4.3 ANN (2, 4, 1) configuration

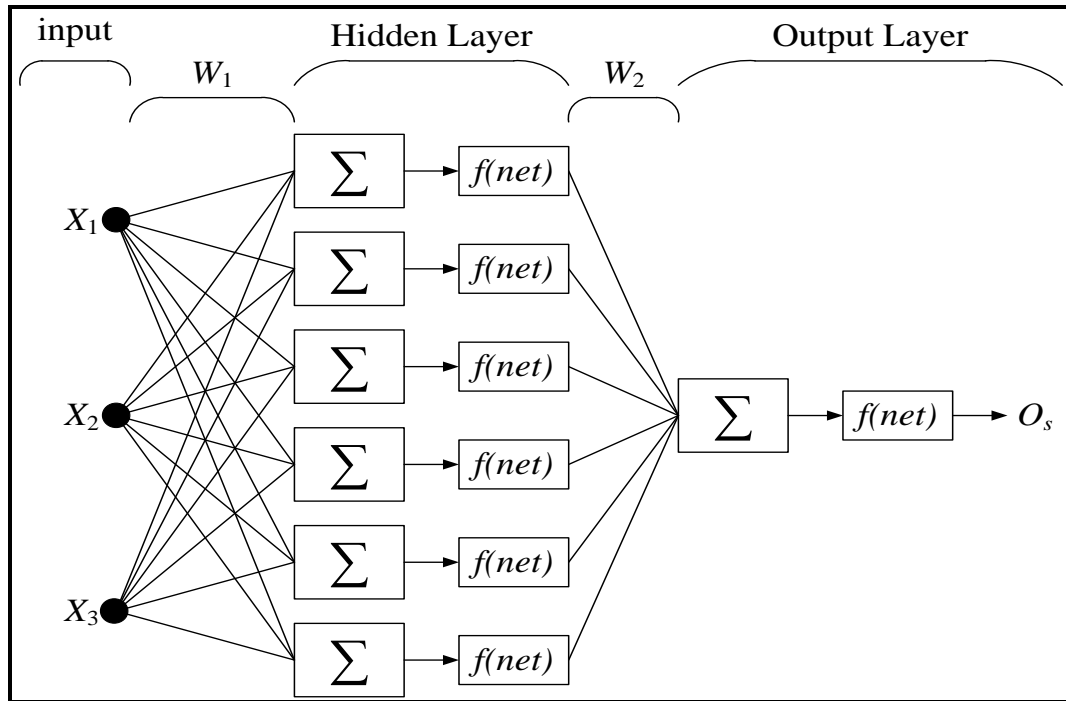


Figure 4.4 ANN (3, 6, 1) configuration

4.1.3 Sigmoid Activation Function

Equation (4.5) is the activation function for the network and it is also called the transfer function. It basically determines the relation between the inputs and outputs of a node and a network. There are some other functions like hyperbolic function, cosine function, and linear functions. The sigmoid activation function is easy to differentiate and usually applied to applications whose desired output values are between 0 and 1. Because of that, this function is usually preferred over other types of activation functions. Figure 4.5 shows the sigmoid activation function.

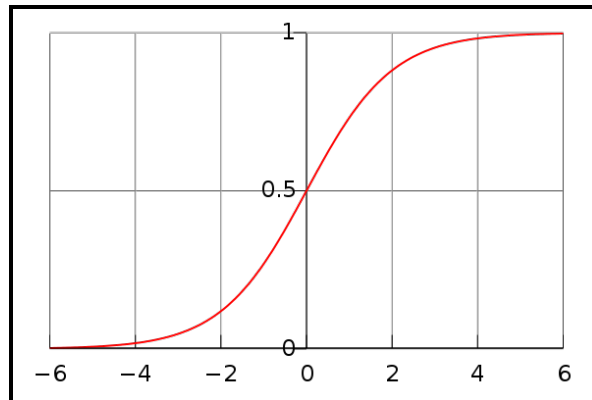


Figure 4.5 Log-Sigmoid Function

4.1.4 ANN Training Performance

The training performance is evaluated using the following performance measures, namely the Mean Square Error (MSE). The main objective of the back-propagation algorithm is to minimize this error by adjusting the weight of the neurons. Initially, the error will be high because the weights are randomly assigned. Throughout the training process, this error decreases and converges to minimum value. Below is the equation for the MSE.

$$E = \sum [F(t) - O(t)]^2 \quad (4.6)$$

Where $F(t)$ is the actual failure of the component (input to the network), and $O(t)$ is calculated failure of the component (output of the network).

4.1.5 Results and Discussion (Bleed Air Regulator-Flight Hour)

In this work, MATLAB was used to write a code to build the network. Table 4-1 shows the calculations for the BAR with different network structures. Before the results are discussed, it is important to consider some of the network parameters that are usually tweaked and adjusted in order to come up with optimum results that come to a close proximity with the actual data. These parameters are:

1. Network structure: It is a vital step to calculate and build a suitable network for our data, the number of neuron and layers are the most significant parameters that will drastically affect accuracy. We will start with two neurons for the input layer, four neurons for the hidden layer, and a single output layer with one neuron. This structure is called (2,4,1). From literature review it was found that in many circumstances, having the number of neurons for the hidden layer equal to double the number on neurons at the input layer gives optimum results. Accordingly, the following network structures will also be investigated (3, 6, 1), (4, 8, 1), and (4, 10, 1). It was obvious that the number of neurons at the hidden layer has a significant effect on the results. Increasing the number of neurons in the hidden layer is the most significant factor that affects the accuracy of result. On the other hand, the input and output layer parameters do not have a major impact on the simulations process.
2. Rate of learning: The back-propagation algorithm provides an approximation to the trajectory in weight spaced computed by the method of steepest descend [33].

The smaller the learning rate, the smaller the changes to the synaptic weights in the network will be from one iteration to the next, and the smoother will be the trajectory in weight spaces, keeping in mind that this is achieved at the cost of a slower rate of learning. On the other hand, if the leaning rate parameter is increased to accelerate the rate of learning, the resulting large changes in the synaptic weights will make the network unstable.

Typically, in most practical applications, learning rate is chosen to be in between 0.1 and 0.3. The number of training epochs is set to a very high value ranging from 1000 to 10000. The training is stopped when the 'mean squared value' of error reduces to a value less than the acceptable threshold or when all the training cycles are completed.

3. Momentum constant: In back-propagation networks, the weight change is in a direction that is a combination of a current gradient and the previous gradient. This approach is beneficial when some training data are very different from a majority of the data. Based on that concept, a small training rate is used in order to avoid a major disruption of the direction of learning when there is unusual pair of training pattern. If the momentum is added to the weight updated formula, the convergence is faster. The weights from previous training must be saved to use the momentum. The main purpose of the momentum is to accelerate the convergence of error propagation algorithm. This method makes the current weights adjustment with a fraction of recent weights adjustment. The momentum constant is between values 0 to 1.

Table **4-1** shows the major outputs for the ANN outputs. Figure **4.6**, Figure **4.7**, Figure **4.8**, and Figure **4.9** show the network output compared to the actual data and the Weibull method.

Table 4-1 Bleed Air Regulator with different ANN structures (FH)

FH	Rank	F(t)	Normalize (Hours)	ANN (4,8,1)	ANN (3,6,1)	ANN (2,4,1)	ANN (4,10,1)
41	1	0.030	0	0.029	0.029	0.053	0.029
262	2	0.073	0.080	0.080	0.189	0.171	0.074
266	3	0.115	0.082	0.113	0.191	0.174	0.110
275	4	0.158	0.085	0.156	0.196	0.181	0.154
295	5	0.201	0.092	0.202	0.204	0.194	0.200
313	6	0.244	0.099	0.239	0.211	0.205	0.232
690	7	0.286	0.236	0.287	0.268	0.318	0.279
821	8	0.329	0.284	0.325	0.337	0.363	0.326
947	9	0.372	0.330	0.367	0.381	0.357	0.378
1233	10	0.415	0.434	0.417	0.427	0.490	0.422
1315	11	0.457	0.463	0.454	0.461	0.499	0.458
1384	12	0.500	0.489	0.499	0.496	0.502	0.496
1454	13	0.543	0.514	0.544	0.532	0.524	0.531
1565	14	0.585	0.554	0.588	0.587	0.598	0.570
1725	15	0.628	0.613	0.623	0.655	0.664	0.630
1750	16	0.671	0.622	0.644	0.664	0.665	0.666
2016	17	0.714	0.718	0.718	0.733	0.772	0.729
2031	18	0.756	0.724	0.754	0.737	0.782	0.741
2234	19	0.799	0.798	0.801	0.819	0.823	0.796
2237	20	0.842	0.799	0.816	0.821	0.823	0.832
2400	21	0.885	0.858	0.848	0.883	0.875	0.897
2669	22	0.927	0.956	0.928	0.907	0.940	0.926
2790	23	0.970	1.000	0.970	0.966	0.965	0.967

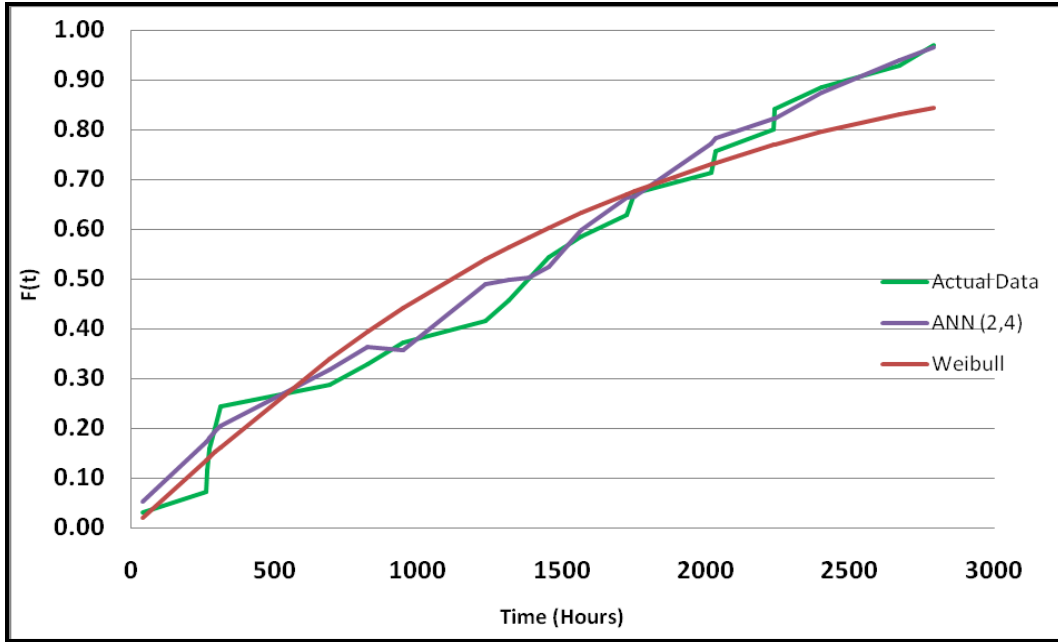


Figure 4.6 BAR (FH) ANN (2, 4, 1) comparison with actual data and Weibull

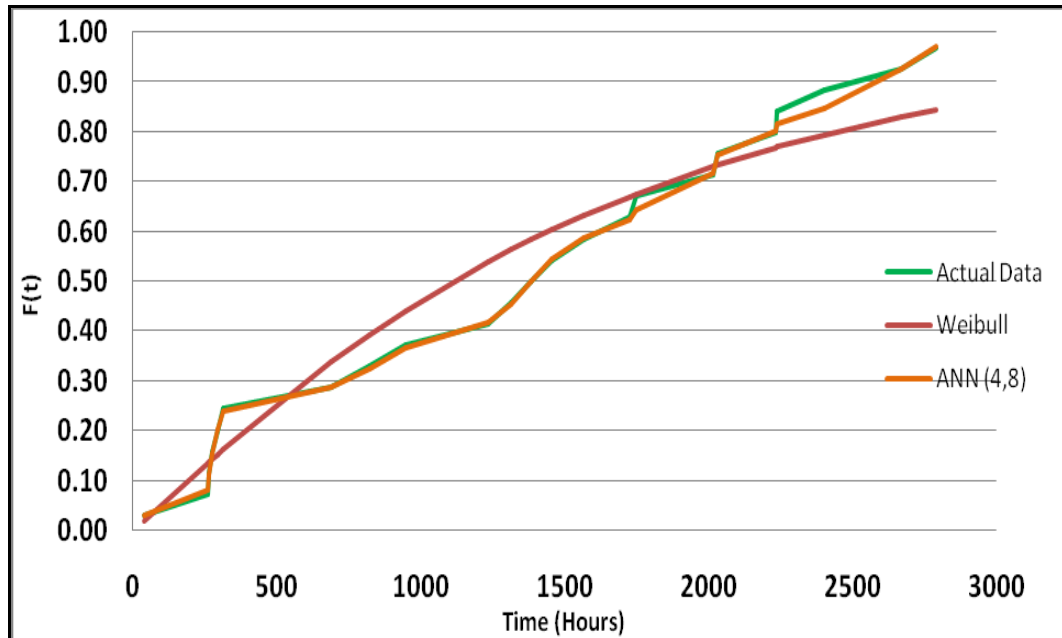


Figure 4.7 BAR (FH) ANN (4, 8, 1) comparison with actual and Weibull data

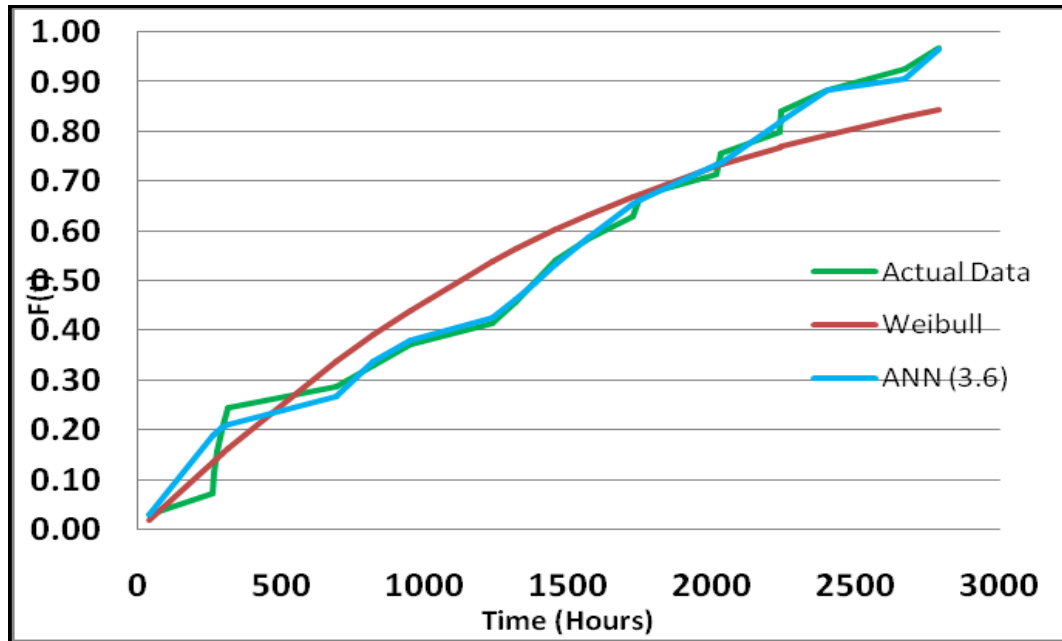


Figure 4.8 BAR (FH) ANN (3, 6, 1) comparison with actual and Weibull data

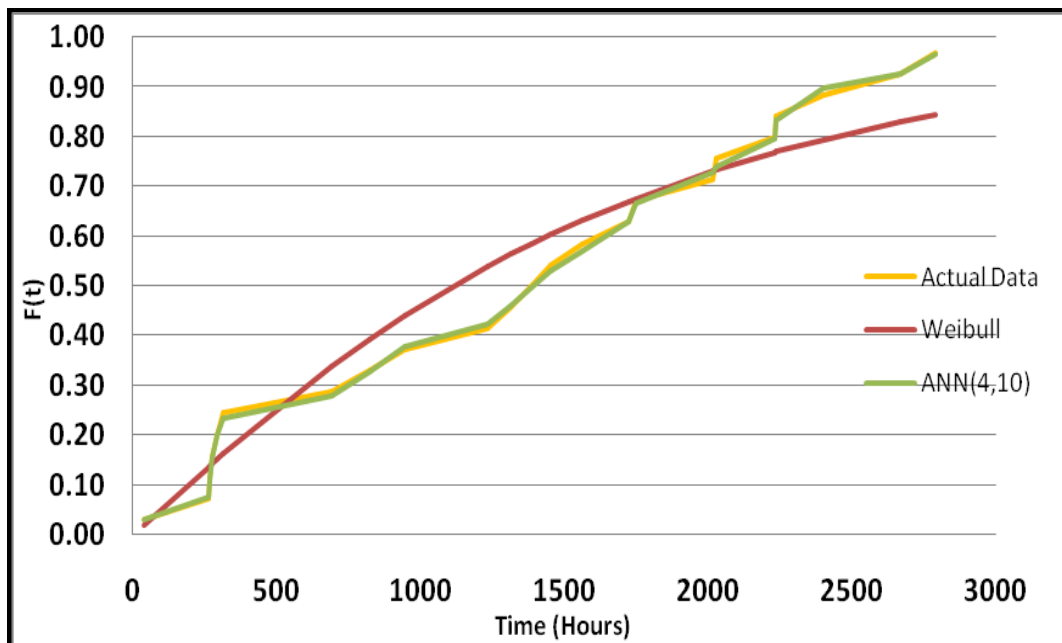


Figure 4.9 BAR (FH) ANN (4, 10, 1) comparison with actual and Weibull data

The average percentage differences of the output failure rate compared to the actual failure data are found to be 16.57%, 13.15%, 1.63%, and 1.62% for ANN having (2,4,1), (3,6,1),(4,8,1) and (4,10,1) configuration respectively. It is evident from the percentage differences that the ANN results improve as the number of inputs and intermediate neurons increase up to four inputs, however, increasing the number of inputs beyond four does not have a significant impact on our calculations. Adjusting other parameters like the learning rate and momentum constant did not indicate any noticeable effect on the accuracy of the network output. Therefore, (4, 8, 1) ANN model has been adapted for the present study. All network parameters are listed in Table 4-2.

Table 4-2 Major network parameters

Parameters	
Network architecture	(4, 8, 1)
Network leaning rate	0.2
Network momentum constant	0.05

4.1.6 Results and Discussion (Bleed Air Regulator-Flight Cycle)

The same procedures will be followed to predict the failure rate for the bleed air regulator in terms of flight cycles (FC). Table 4-3 shows the failure data with all required calculations and outputs to estimate the failure by utilizing neural networks.

Table 4-3 Bleed air regulator with different ANN structures (FC)

(FC)	Rank	F(t)	Normalized	ANN(2,4,1)	ANN (3,6,1)	ANN(4,8,1)
76	1	0.030	0.000	0.065	0.051	0.066
345	2	0.073	0.063	0.165	0.161	0.097
394	3	0.115	0.075	0.186	0.180	0.128
396	4	0.158	0.075	0.187	0.181	0.159
462	5	0.201	0.091	0.214	0.203	0.203
517	6	0.244	0.104	0.233	0.218	0.239
1104	7	0.286	0.242	0.310	0.279	0.300
1215	8	0.329	0.268	0.346	0.316	0.328
1461	9	0.372	0.326	0.412	0.386	0.370
1897	10	0.415	0.429	0.453	0.434	0.420
2001	11	0.457	0.453	0.485	0.463	0.458
2053	12	0.500	0.466	0.504	0.481	0.495
2209	13	0.543	0.502	0.565	0.543	0.550
2329	14	0.585	0.531	0.603	0.587	0.591
2395	15	0.628	0.546	0.619	0.608	0.619
2512	16	0.671	0.574	0.641	0.636	0.651
2981	17	0.714	0.684	0.755	0.735	0.735
2984	18	0.756	0.685	0.756	0.736	0.757
3271	19	0.799	0.752	0.807	0.799	0.800
3495	20	0.842	0.805	0.838	0.828	0.841
3739	21	0.885	0.863	0.891	0.873	0.889
4097	22	0.927	0.947	0.947	0.950	0.929
4322	23	0.970	1.000	1.000	0.985	0.971

Figures 4.10,4.11,4.12,4.13 show all ANN results with a comparison to the Weibull method.

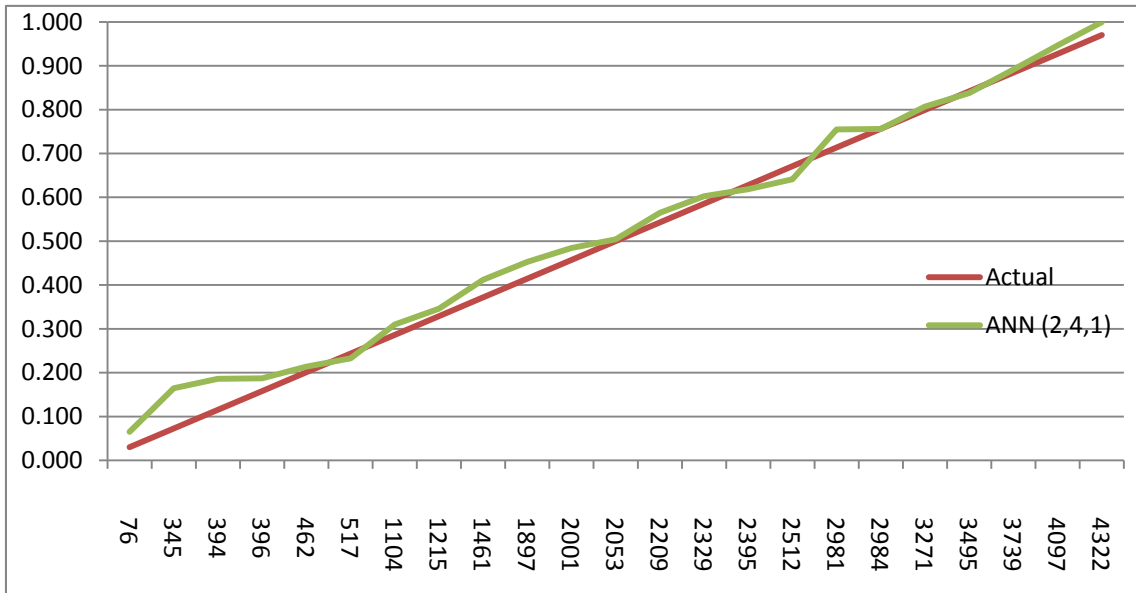


Figure 4.10 BAR ANN (2,4,1) compared to the actual (FC)

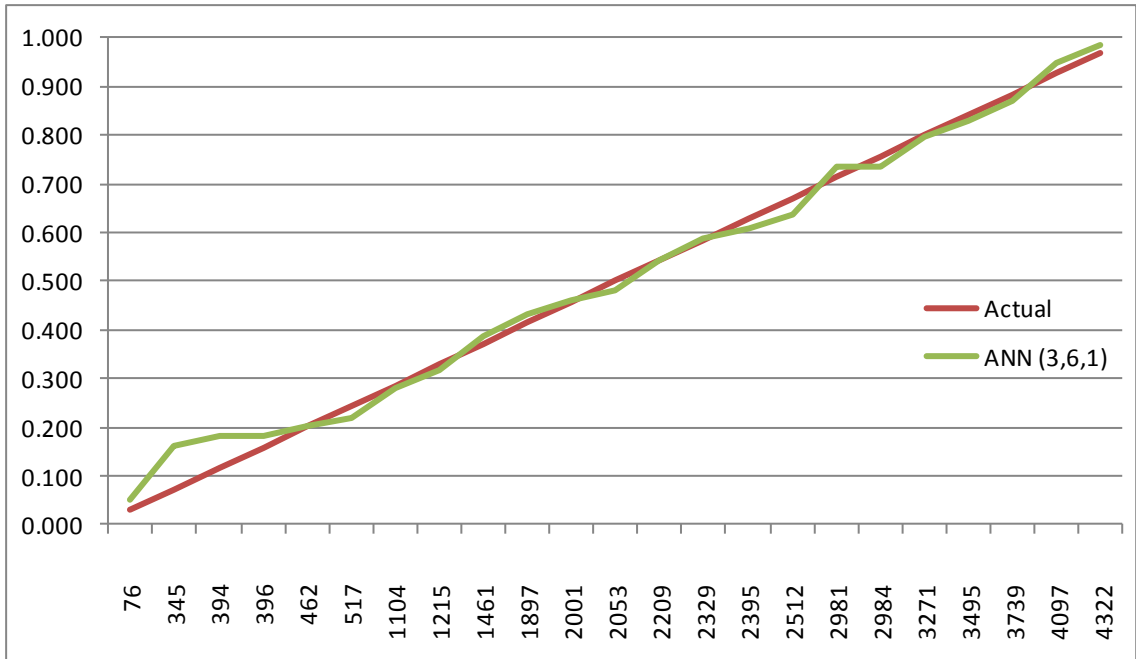


Figure 4.11 BAR ANN (3,6,1) compared to actual (FC)

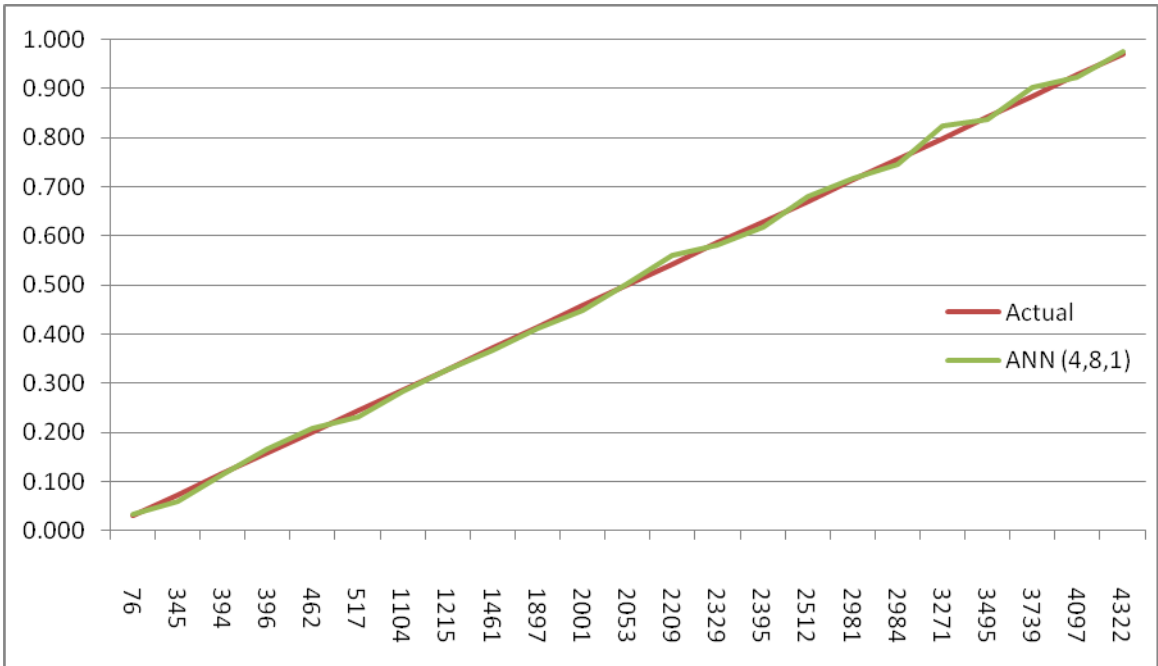


Figure 4.12 BAR ANN (4,8,1) compred to actual (FC)

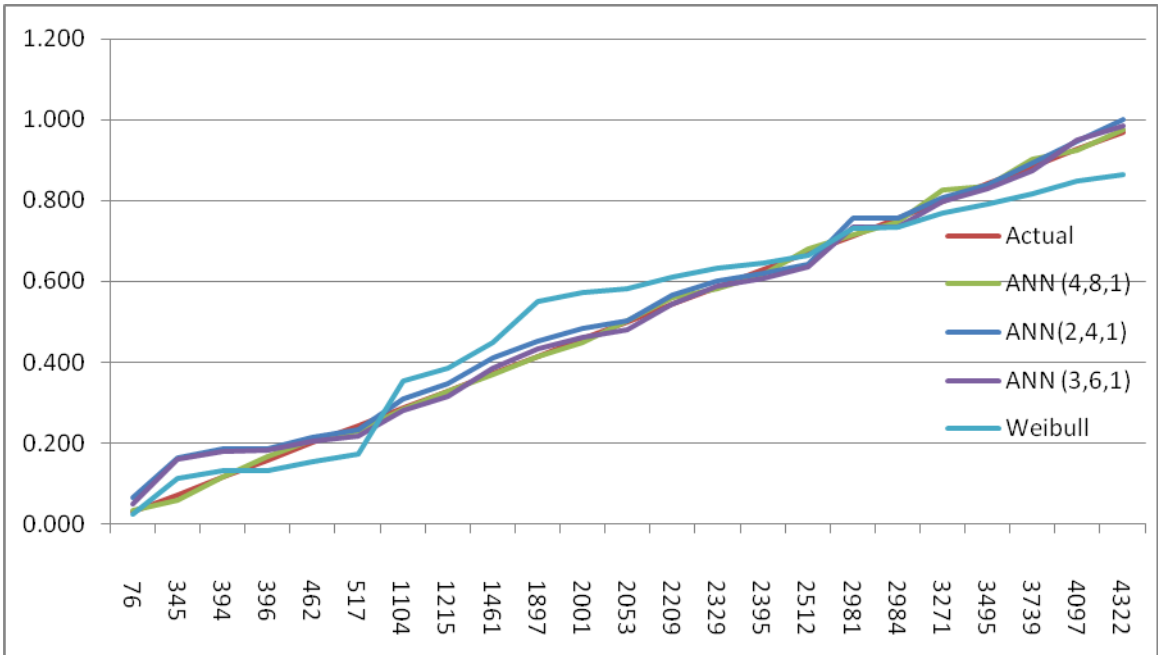


Figure 4.13 BAR ANN results compared to actual and Weibull (FC)

Table 4-4 shows the percentage error for all ANN configurations and Weibull compared to actual data.

Table 4-4 High bleed air regulator results percentage error (FC) compared to actual data

Curve	Mean Percentage Error (compared to F(t))
Weibull	15.38
ANN (2,4,1)	10.30
ANN (3,6,1)	8.68
ANN (4,8,1)	2.81

From the above table, it can be clearly observed that ANN with (4, 8, 1) configuration has the most accurate output. The network training is drastically improved with minimum change to the network structure. On the other hand, Weibull method showed a significant error when compared to the neural network method.

4.1.7 Results and Discussion (HSV- FH)

Following the BAR analysis and calculations procedures, the high stage valve data output did show that the ANN accuracy was not really affected by the size of the data. As a start, the same ANN configuration structure was followed with the same network parameters, the final output was very close compared to the actual data. To ensure a proper simulation, some network parameters were tweaked to study the effect of those parameters on the network performance. No significant results were noticed which in turn

shows the strength of the ANN approach in terms of the network learning even with small data. Table 4-5 shows summary of high stage valve calculations with different ANN structures.

Table 4-5 High stage valve with different ANN structure (FH)

FH	Rank	F(t)	CDF	NORMALIZED	ANN (4,8,1)	ANN (3,6,1)	ANN (2,4,1)
234	1	0.049	0.066	0.000	0.049	0.102	0.0828
236	2	0.118	0.067	0.001	0.117	0.103	0.0834
500	3	0.188	0.179	0.107	0.252	0.180	0.1848
760	4	0.257	0.298	0.212	0.256	0.241	0.2553
989	5	0.326	0.400	0.305	0.310	0.335	0.337
1022	6	0.396	0.414	0.318	0.396	0.346	0.3608
1211	7	0.465	0.492	0.394	0.496	0.472	0.4648
1641	8	0.535	0.645	0.568	0.535	0.592	0.6099
1786	9	0.604	0.688	0.626	0.608	0.645	0.6494
1901	10	0.674	0.720	0.673	0.674	0.675	0.6899
1923	11	0.743	0.725	0.682	0.716	0.687	0.702
2100	12	0.813	0.768	0.753	0.812	0.823	0.8262
2155	13	0.882	0.780	0.775	0.881	0.849	0.855
2712	14	0.951	0.876	1.000	0.951	0.947	1.0103

The following graphs demonstrate the output of our simulation process with a comparison to the Weibull to the ANN analysis for the high stage valve (FH).

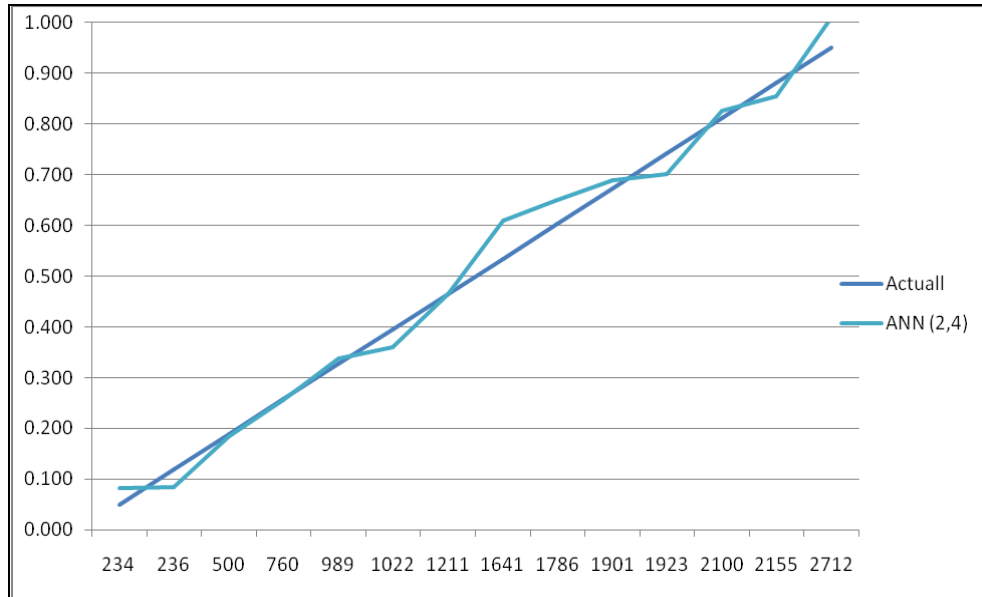


Figure 4.14 High stage valve (FH) ANN (2, 4, 1) compared to actual data

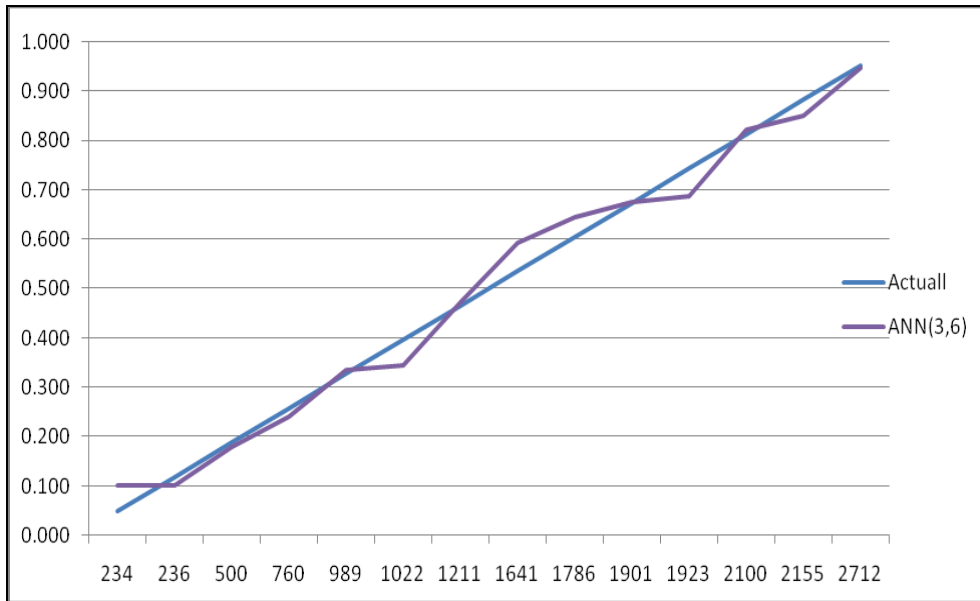


Figure 4.15 High stage valve (FH) ANN (3, 6, 1) compared to actual data

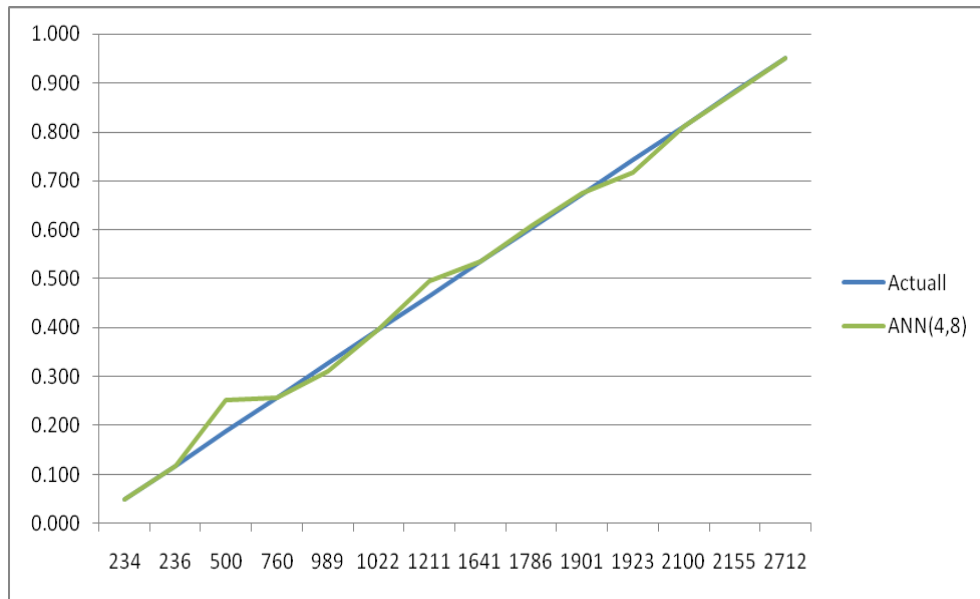


Figure 4.16 High stage valve (FH) ANN (4, 8, 1) compared to actual data

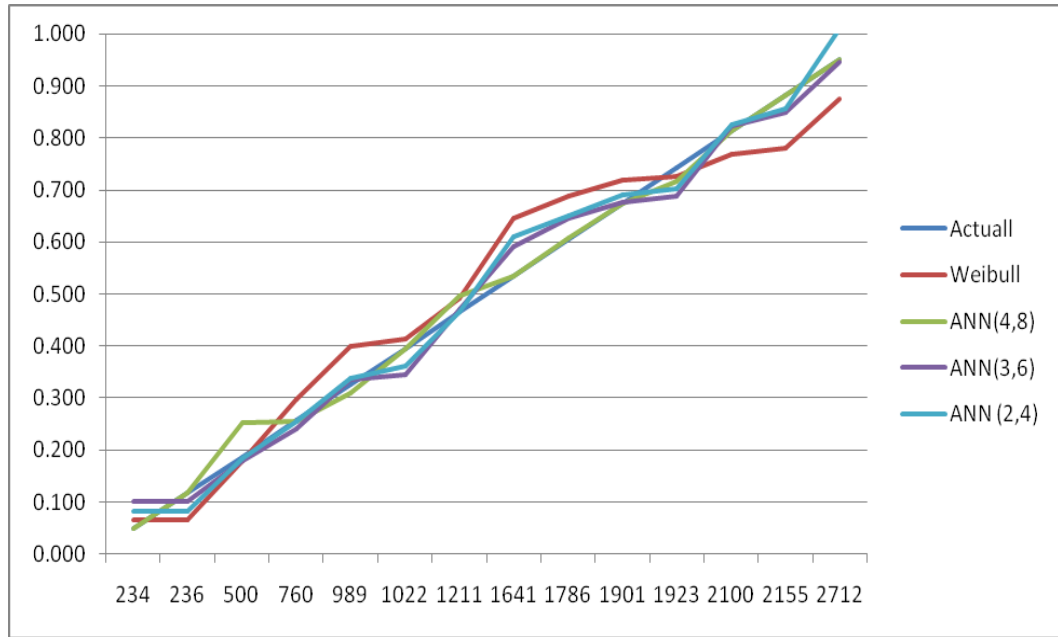


Figure 4.17 High stage valve (FH) ANN compared to actual and Weibull

It is clear from above graphs that the most optimum ANN configuration structure for the simulation process is (4, 8, and 1). Table 4-6 shows the deviation of each curve (percentage error) from the actual data.

$$\text{Percentage error} = \text{Abs} ((\text{Calculated} - \text{Actual}) / \text{Calculated})$$

Table 4-6 High stage valve average percentage error (FH) compared to actual data

Curve	Mean Percentage Error (compared to F(t))
Weibull	15.39
ANN (2,4,1)	9.72
ANN (3,6,1)	9.02
ANN (4,8,1)	3.02

4.1.8 Results and Discussion (HSV-FC)

All figures and tables below show the output for ANN simulation for high stage valve (cycles). The same approach used for the (hours) analysis was exactly followed to generate the following results in Table 4-7:

Table 4-7 high stage valve (cycles) with different ANN structures

t(FC)	Rank	F(t)	CDF	Normalized	ANN(2,4,1)	ANN(3,6,1)	ANN(4,8,1)
337	1	0.049	0.064	0.000	0.054	0.115	0.050
346	2	0.118	0.066	0.002	0.055	0.115	0.117
930	3	0.188	0.226	0.162	0.188	0.190	0.188
1014	4	0.257	0.250	0.185	0.188	0.220	0.253
1510	5	0.326	0.388	0.320	0.326	0.340	0.327
1655	6	0.396	0.426	0.360	0.344	0.381	0.393
1890	7	0.465	0.484	0.424	0.464	0.470	0.445
2707	8	0.535	0.657	0.647	0.539	0.640	0.575
2806	9	0.604	0.675	0.674	0.620	0.672	0.608
3235	10	0.674	0.743	0.791	0.704	0.721	0.690
3238	11	0.743	0.744	0.792	0.718	0.721	0.747
3311	12	0.813	0.754	0.812	0.784	0.729	0.812
3744	13	0.882	0.809	0.930	0.787	0.885	0.873
4000	14	0.951	0.836	1.000	0.999	0.961	0.951

The following graphs demonstrate the output of our simulation process with a comparison to the Weibull to the ANN analysis for the high stage valve (cycles).

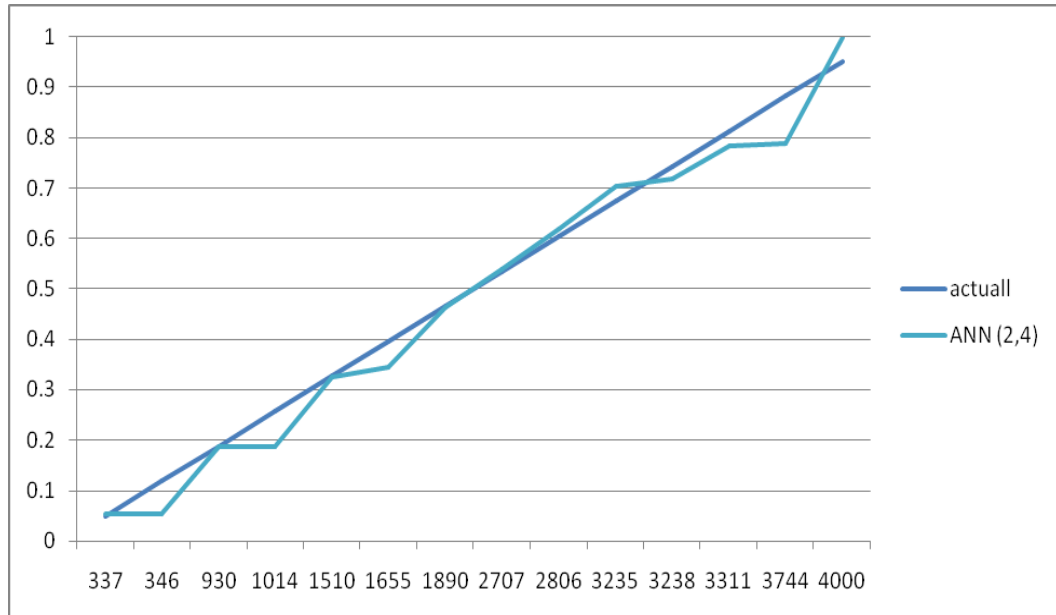


Figure 4.18 High stage valve (FC) ANN (2,4,1) compared to actual data

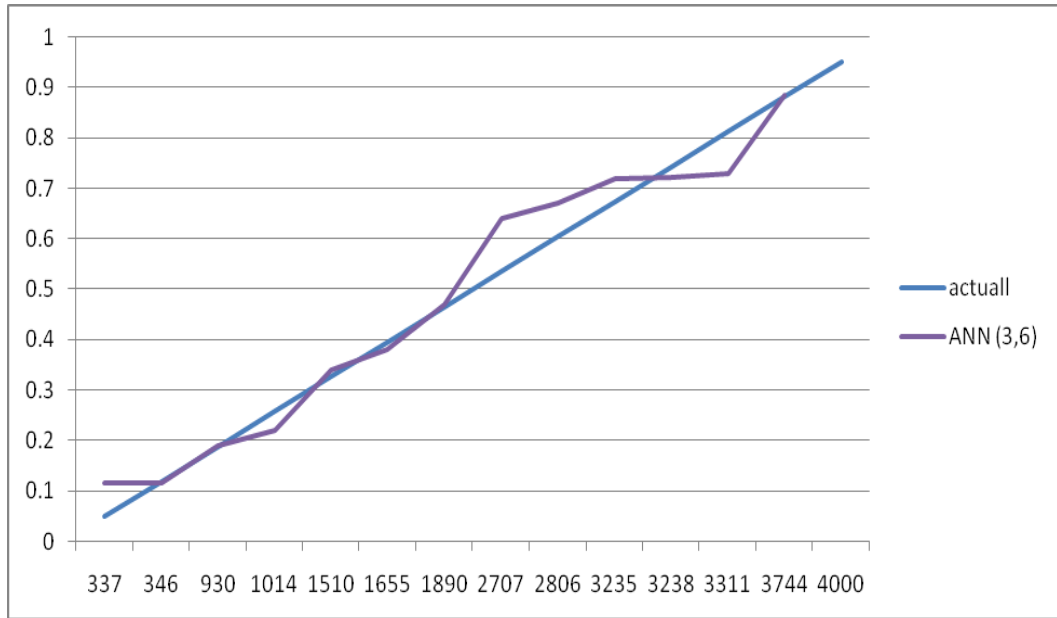


Figure 4.19 High stage valve (FC) ANN (3,6,1) compared to actual data

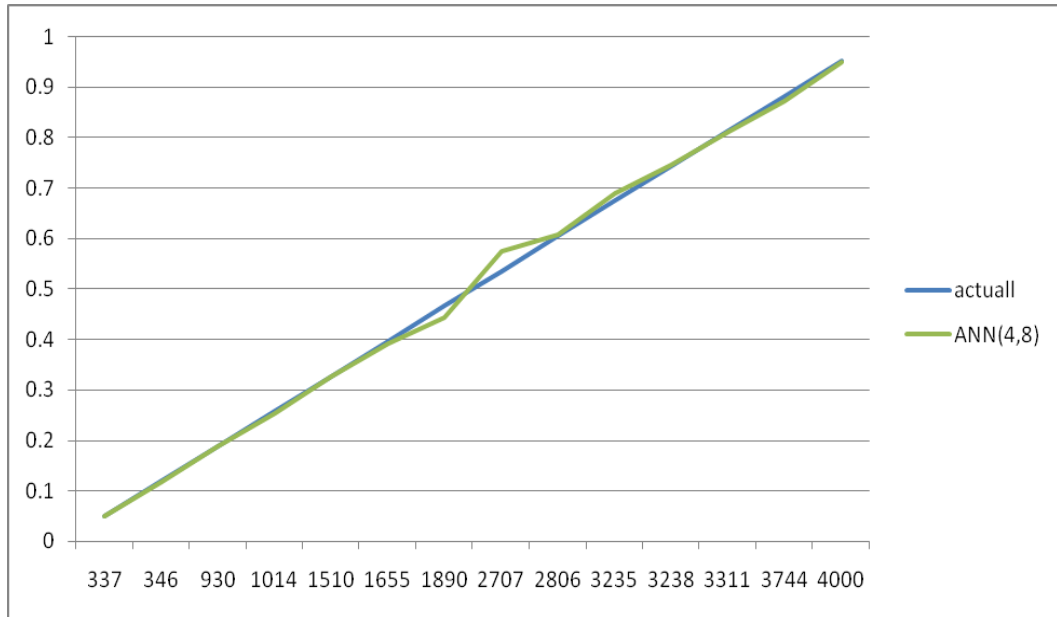


Figure 4.20 High stage valve (FC) ANN (4,8,1) compared to actual data

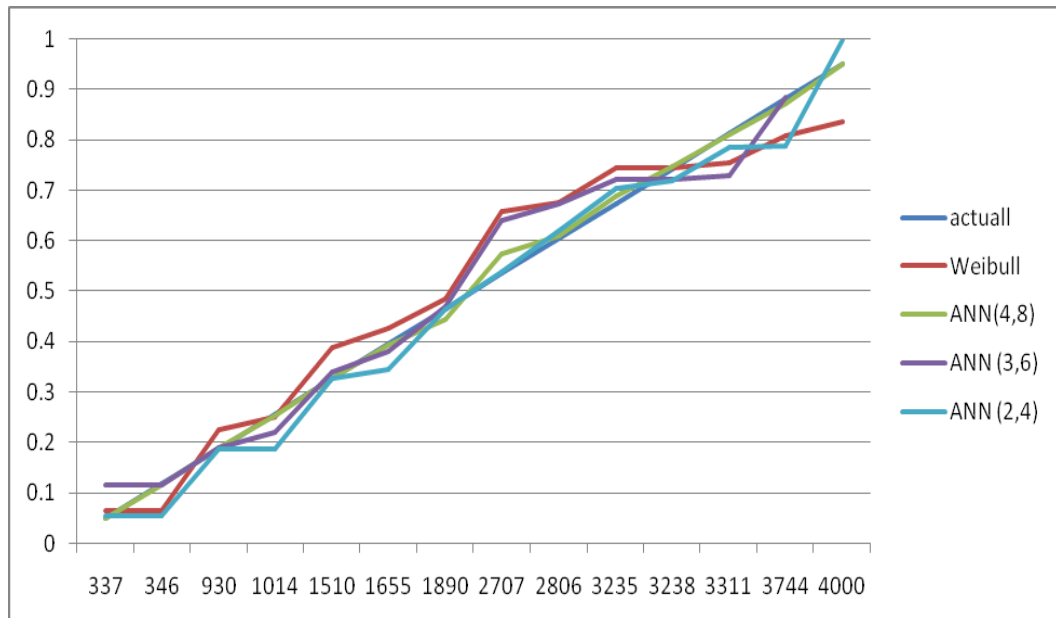


Figure 4.21 High stage valve (FC) ANN compared to actual data and Weibull

It is clear from above graphs that the most optimum ANN configuration structure for the simulation process is (4, 8, and 1). Table 4-8 below shows how far each curve (percentage error) from the actual data.

Table 4-8 Stage valve average percentage error (FC) compared to actual data

Curve	Mean Percentage Error (compared to F(t))
Weibull	15.16
ANN (2,4,1)	15.01
ANN (3,6,1)	9.70
ANN (4,8,1)	1.59

4.1.9 Results and Discussion (PRSOV-FH)

Following the same approach used for the rest of the components, ANN analysis is conducted to simulate the failure prediction for the PRSOV valve. It is evident that Weibull model accuracy level was affected by the number of data for this valve. For ANN results reliability, the prediction analysis for this valve will show how ANN behaves with limited number of data. It should be emphasized that because the valves at hand are critical parts of the airplane propulsion system, the reliability of all predictions should be accurate enough to ensure high safety standard for all flight operation conditions. Table 4-9 shows all ANN analysis for PRSOV in terms of flight hours (FH).

Table 4-9 ANN results for PRSOV (FH)

t (FH)	Rank	F(t)	CDF	Normalized	ANN (2,4,1)	ANN (3,6,1)	ANN (4,8,1)
77	1	0.061	0.038	0.000	0.046	0.046	0.061
427	2	0.149	0.236	0.176	0.145	0.157	0.149
512	3	0.237	0.282	0.219	0.142	0.222	0.237
954	4	0.325	0.488	0.441	0.379	0.325	0.325
1036	5	0.412	0.521	0.483	0.421	0.392	0.412
1117	6	0.500	0.551	0.523	0.472	0.484	0.500
1256	7	0.588	0.599	0.593	0.567	0.622	0.593
1340	8	0.675	0.626	0.636	0.631	0.668	0.675
1360	9	0.763	0.633	0.646	0.624	0.675	0.729
1990	10	0.851	0.786	0.963	0.899	0.866	0.851
2064	11	0.939	0.799	1.000	0.935	0.921	0.939

Figures (4-22), (4-23),(4-24), and (4-25) show output of our simulation process with a comparison to the Weibull to the ANN analysis for the PRSOV valve (FH).

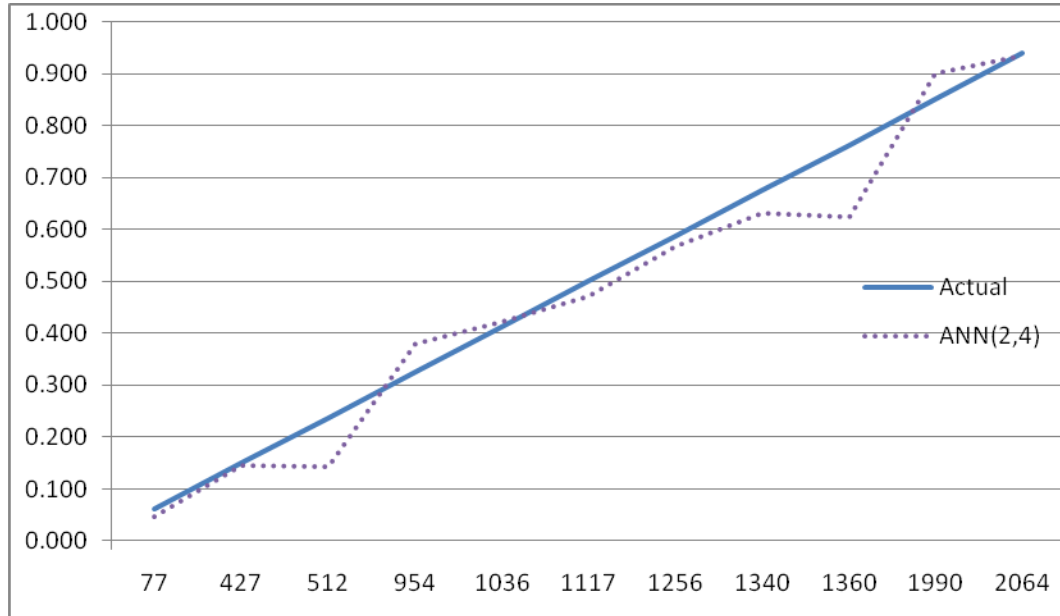


Figure 4.22 PRSOV (FH) ANN (2,4,1) comparison with actual data

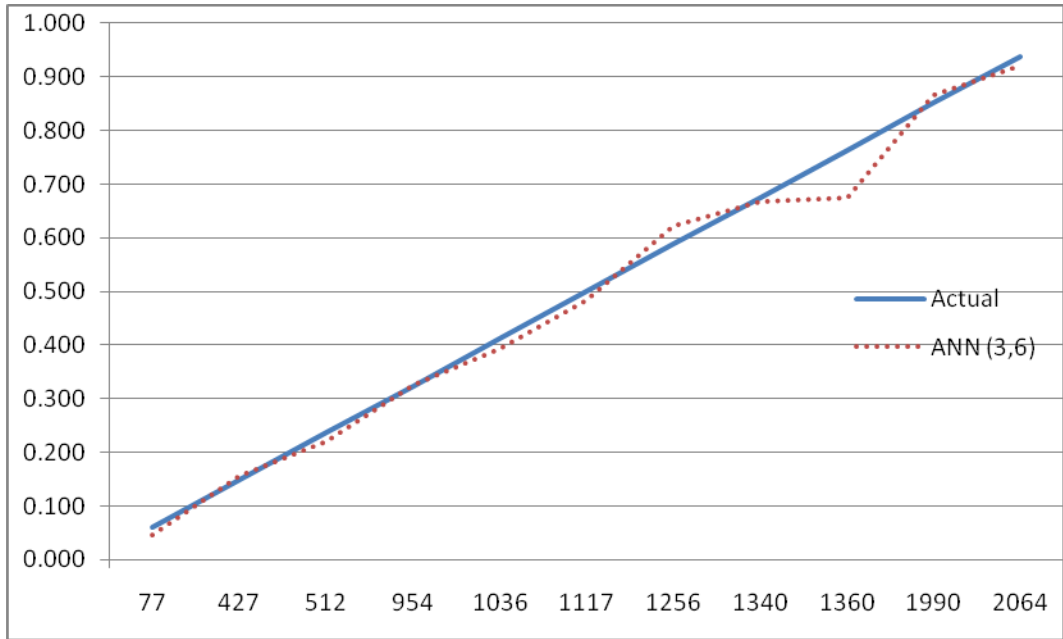


Figure 4.23 PRSOV (FH) ANN (3,6,1) comparison with actual data

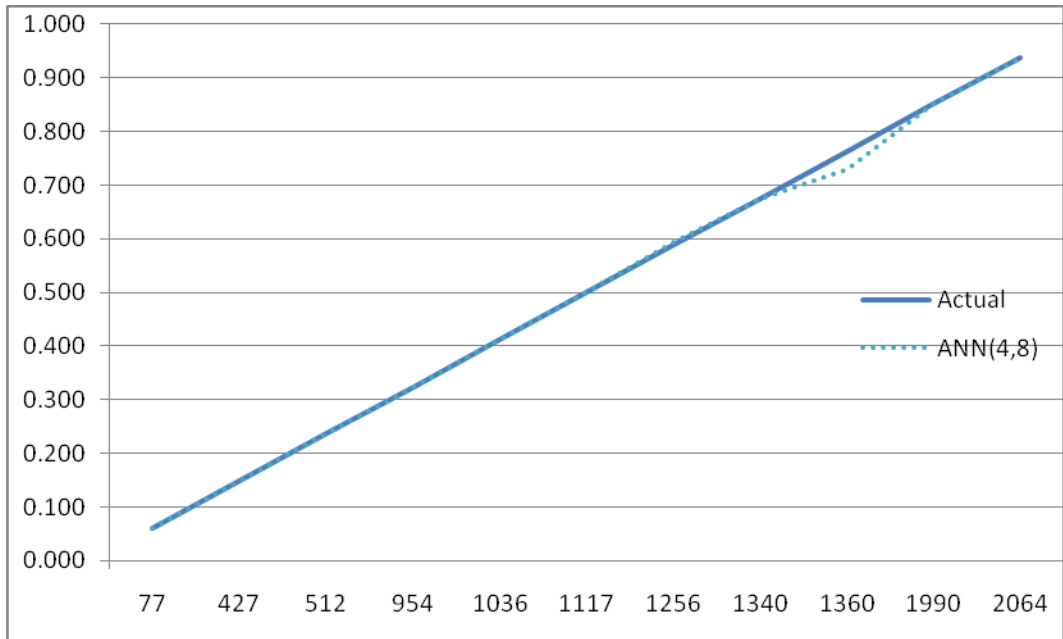


Figure 4.24 PRSOV (FH) ANN (4,8,1) with actual data

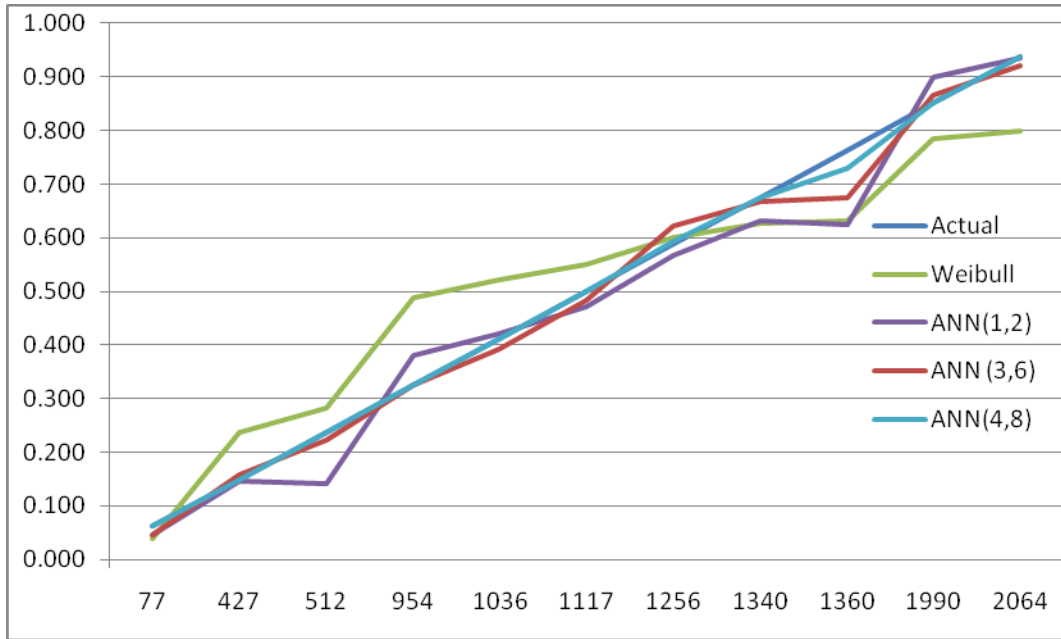


Figure 4.25 PRSOV (FH) ANN compared with Weibull

Based on the above figures, it can be concluded that network with (4, 8, 1) configuration gives the best results compared to the actual failure rates. Despite limited number of observations, ANN analysis showed a strong agreement with actual data as shown in Table 4-10.

Table 4-10 PRSOV analysis percentage error compared to actual data (FH)

Curve	Mean Percentage Error
Weibull	21.29
ANN (2,4,1)	14.86
ANN (3,6,1)	7.05
ANN (4,8,1)	0.51

Table 4-10 shows the power of neural network in terms of accuracy. Although the data size was relatively small, the output was extremely in close proximity with the actual failure rate, which indicates the reliability of the ANN for prediction analysis.

4.1.10 Results and Discussion (PRSOV-FC)

As mentioned before, the power of the neural network approach could be clearly seen with the PRSOV due to the limited number of observations. The model is tested with small sample of data compared to other valves. The following figures are the output of the neural network model simulation for the PRSOV in terms of flight cycles (FC) with the same configuration and parameters.

Similar to the flight hour's analysis, Table 4-11 shows the main calculations and outputs for the PRSOV in terms of (FC).

Table 4-11 ANN results for PRSOV (FC)

t (FC)	Rank	F(t)	Normalized	ANN(2,4,1)	ANN(3,6,1)	ANN(4,8,1)
112	1	0.061	0.000	0.067	0.028	0.061
720	2	0.149	0.200	0.267	0.237	0.169
781	3	0.237	0.221	0.309	0.264	0.237
1605	4	0.325	0.492	0.597	0.530	0.325
1625	5	0.412	0.499	0.613	0.546	0.430
1725	6	0.500	0.532	0.698	0.645	0.500
1769	7	0.588	0.546	0.724	0.692	0.588
1806	8	0.675	0.559	0.738	0.729	0.676
1891	9	0.763	0.587	0.747	0.799	0.763
2093	10	0.851	0.653	0.826	0.830	0.851
3145	11	0.939	1.000	1.238	1.058	0.939

Figures 4-26, 4-27, 4-28 and 4-29 illustrate all ANN outputs following the same approach and parameters for the flight hour's calculations.

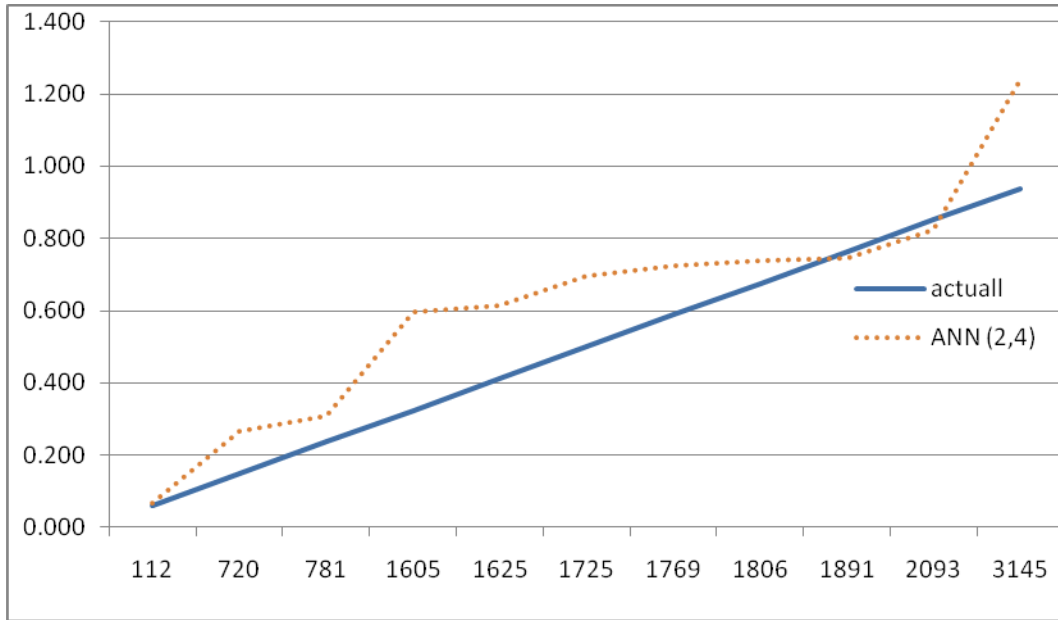


Figure 4.26 PRSOV (FC) ANN (2,4,1) comparison with actual data

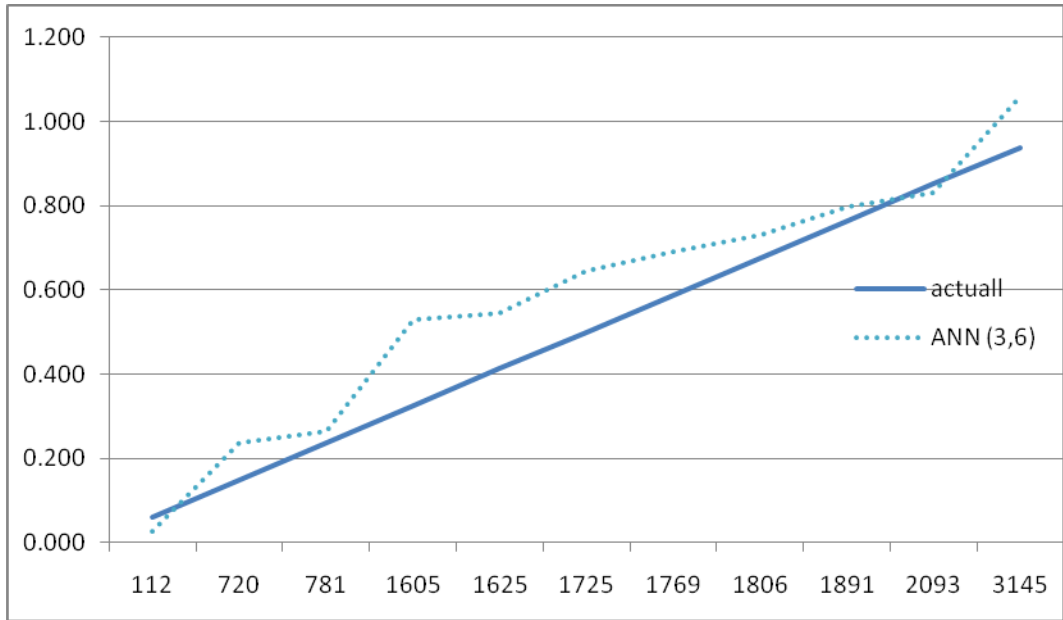


Figure 4.27 PRSOV (FC) ANN (3, 6, 1) comparison with actual data

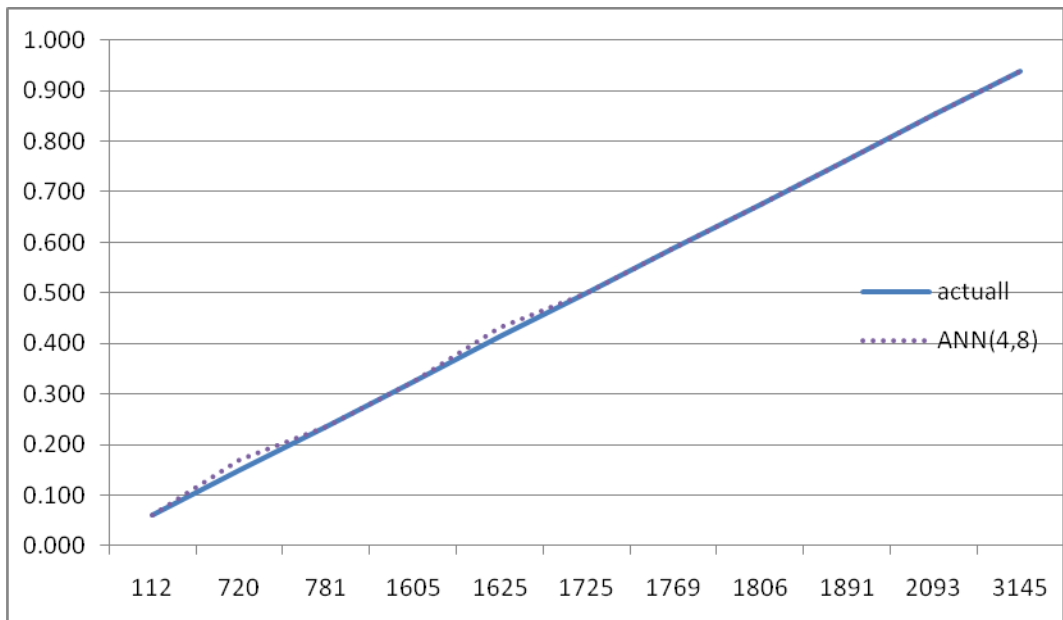


Figure 4.28 PRSOV (FC) ANN (4,8,1) comparison with actual data

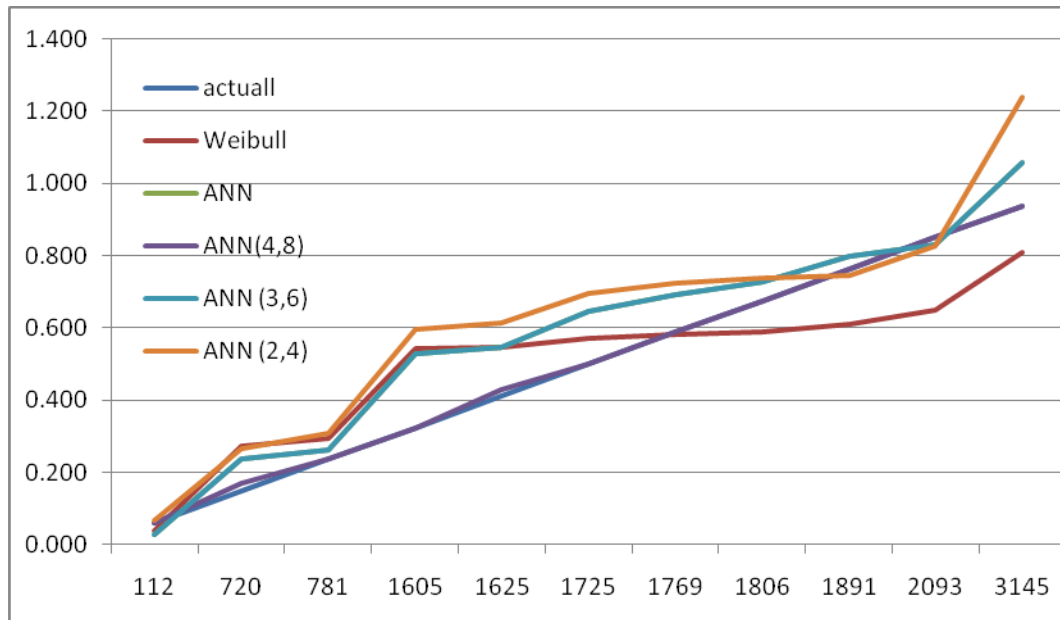


Figure 4.29 PRSOV ANN comparison with Weibull

Based on the above figures, it can be easily noted that (4, 8, 1) configuration gives the best results compared to the actual failure rates. Although there is limited number of failure data, this configuration results showed a strong agreement with the actual failure data. Table 4-12 shows a comparison of Weibull and ANN to the actual data.

Table 4-12 PRSOV analysis percentage error compared to actual data (FC)

Curve	Mean Percentage Error (compared to F(t))
Weibull	25.69
ANN (2,4,1)	21.68
ANN (3,6,1)	26.98
ANN (4,8,1)	1.43

From the above table, it is clear that ANN performance and accuracy is less than the results for the flight hours. However, there is a big improvement in the training process if compared the (3, 6, 1) network to the (4, 8, 1) one. Referring to the (4,8,1) graph, it can be observed that the network was showing a fluctuation results for the early failures, but when the valve gets mature, a considerable enhancement for the failure prediction is noticed. One particular conclusion is the high accuracy of the non-linearity of the ANN technique compared to the traditional statistical approaches like Weibull.

4.1.11 Results Summary

Table 4-13 and Table 4-14 summarizes all results from Weibull and ANN. The main objective of summarizing the results is to identify all factors that affected the accuracy and performance of both methods. Results will be discussed for flight hours and cycles.

Table 4-13 Results summary for all components (FH)

Component	Number of observations	ANN (2,4,1) Error (%)	ANN (3,6,1) Error (%)	ANN (4,8,1) Error (%)	Weibull analysis Error (%)	Most Accurate Result
BAR	23	16.57	13.15	1.63	17.02	1.63
High Stage Valve	14	9.72	9.02	3.02	15.39	3.02
PRSOV	11	14.86	7.05	0.51	21.29	0.51

As shown in Table 4-13, it can be easily noted that ANN results by far gave the best results in agreement with the actual failure data. Surprisingly, ANN gave the best results with minimum number of observations. That is a powerful aspect of artificial intelligence where networks training can be accurate with limited number of data. On the other hand, Weibull method did not give reliable results. The Weibull method performance was affected by the number of data and shown fluctuating outputs. This is due to the fact that Weibull is a traditional statistical approach that might be severely affected by the data size and nonlinearity.

The highest error for the ANN method was at the high stage valve where the network struggled with the training especially for pre mature failures. This is basically due to a couple of mature failures of the valve in the beginning. Because of that, the network showed good results with mature failures which are the dominant factor for the high stage valve.

Table 4-14 Results summary for all components (FC)

Component	Number of observations	ANN (2,4,1) Error (%)	ANN (3,6,1) Error (%)	ANN (4,8,1) Error (%)	Weibull analysis Error (%)	Most Accurate Result
BAR	23	10.30	8.68	2.81	15.38	2.81
High Stage Valve	14	15.10	9.7	1.59	15.16	1.59
PRSOV	11	21.68	26.98	1.43	25.96	1.43

Overall, the ANN figures and results showed a strong agreement with the actual failure rates. Moreover, changing the number of neurons in the hidden layer has a significant impact on the network results. The number of failure data for each valve didn't have a visible effect on network performance. On the other hand, the Weibull results were too far from the actual data. Number of failures aggravated and degraded the accuracy of Weibull model.

Chapter 5

ANN MODEL VALIDATION

Before using the developed ANN failure model in maintenance planning, its predictions need to be validated. A partial set of the gathered failure data is used to construct the verification model. Fourteen points, see Table 5.1, covering the bleed air regulator life range to 2392 Flight Cycles are used. The predictions of this model up to 4322 Flight Cycles are compared against actual failure data. Figure 5.1 shows the ANN model results of this reduced data set up to 2392 FC, and Figure 5.2 shows a comparison of the predictions of this model up to 4322 FC with the actual failure data.

Table 5.1. Partial data set for model verification.

(FC)	Rank	F(t)	Normalized	ANN(4,8,1)
76	1	0.049	0.000	0.054
345	2	0.118	0.119	0.155
394	3	0.188	0.141	0.189
396	4	0.257	0.142	0.256
462	5	0.326	0.171	0.337
517	6	0.396	0.196	0.375
1104	7	0.465	0.456	0.470
1215	8	0.535	0.506	0.546
1461	9	0.604	0.615	0.604
1897	10	0.674	0.808	0.683
2001	11	0.743	0.854	0.754
2053	12	0.813	0.877	0.835
2209	13	0.882	0.947	0.879
2329	14	0.951	1.000	0.950

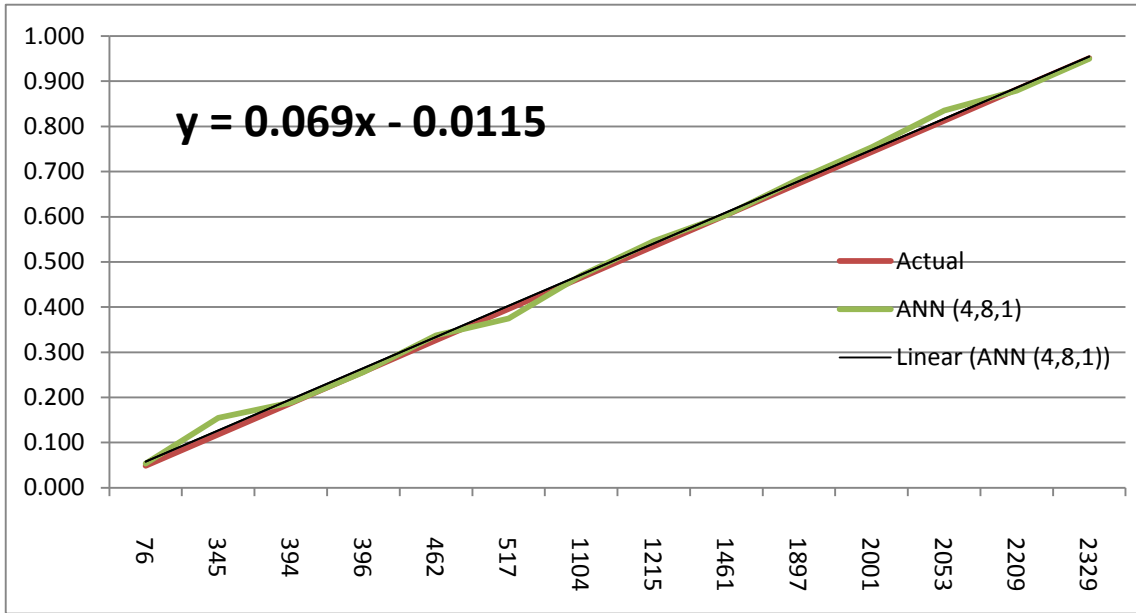


Figure 5.1 BAR (FC) test sample

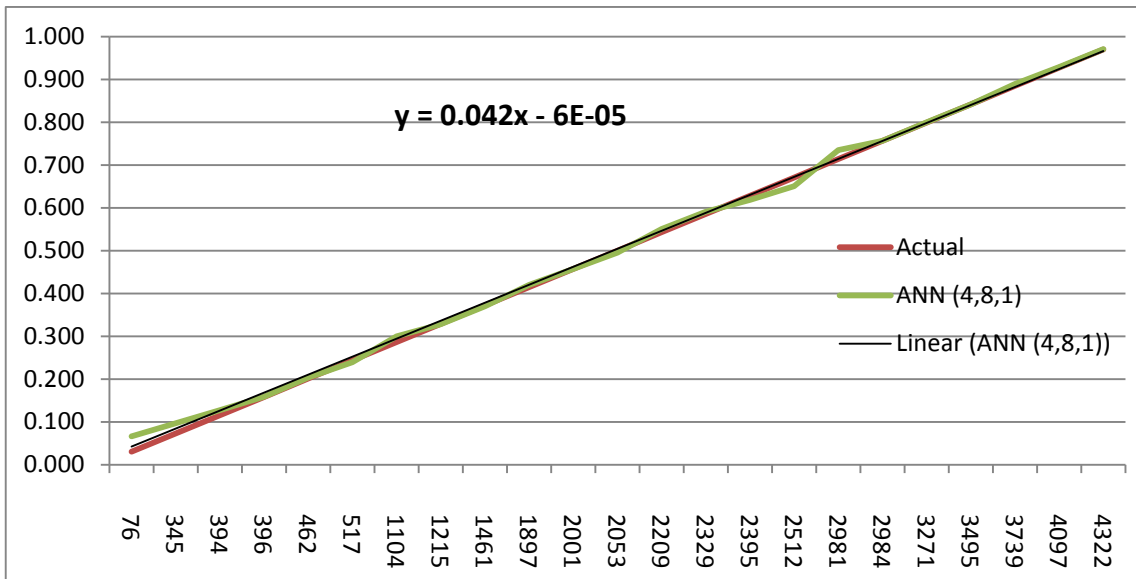


Figure 5.2 BAR (FC) ANN comparison with actual data

As seen from Figure 5.2, there is excellent agreement between the ANN predicted values and the collected failure data. This shows, that with even a small number of gathered data points, neurons, and with just one hidden layer, the model is capable of predicting very accurate failure rates for a number of flight cycles FC that is roughly equal to that of the collected data range. This is a very strong maintenance planning tool, because based on the measured data of, say two years, the failure rate predictions for the following two years could be obtained with excellent accuracy.

Chapter 6

CONCLUSION AND FUTURE WORK

In this work, Weibull model and Artificial Neural Network model were utilized to predict the failure rate of the bleed air system of a Boeing aircraft. For the Weibull analysis, the data was fitted into the model using two parameters. The goodness of fit (GOF) test was performed to all data to check the applicability of the Weibull to the data. Results of the Weibull analysis did not show a strong level of reliability when compared to the actual failure data.

For the ANN analysis, the network was designed with different architecture and parameters to ensure reliable results with strong agreement with actual failure data. It was evident that the network configuration has a crucial impact on the network performance. All parameters were tweaked and adjusted to study the effect of each single element on the behavior of the network. ANN predictions matched very well with the collected failure data and showed a high level of reliability.

To further utilize this work and to better adapt it to support of maintenance strategies, there are several points that can be investigated:

- a. The effect of using other ANN schemes in the simulation, particularly Radial Based Functions, could be investigated and comparison between different schemes would yield valuable information on the best scheme for a particular failure type.
- b. The failure data gathered from the field can be categorized by the season. It is known that hot season got more failures than other seasons. It would be appropriate to check the effect of environmental factors in the reliability of the bleed air system.

- c. The application of this work could be extended into many areas where failure prediction becomes a dilemma. The prediction of failure rate for any component can be calculated using the same approach mentioned in this work. The key is to have an accurate failure history in order to come up with reliable calculations.
- d. Based on the results presented in this work, an optimization procedure could be developed for an efficient preventive maintenance plan. It should take into account the preventive maintenance time and cost, as well as the repair time and cost. Based on the manufacturer acceptable reliability values, the downtime for maintenance could be minimized without compromising the safety of the flight.
- e. This study can be a great tool for spare part inventory planning. Having an accurate failure prediction figures will reduce cost and enhance aircraft availability. The other benefit is to avoid over stocking which in turns decreases the warehouse storage capability.

REFERENCES

1. Weibull, W. (1951). A statistical distribution functions of wide applicability, *J. Appl. Mech.-Trans. ASME* 18, 293–297.
2. Abernethy, R.B., “The New Weibull Handbook”, 4th edition, Abernethy 2000.
3. Zaretsky, E. V. 1987. Fatigue criterion to system design, life and Reliability, *AIAA Journal of Propulsion and Power* 3: 76-83.
4. Al-Garni, A.Z., Ahmed, S.A. & Siddiqui, M. “Modeling failure rate for Fokker F-27 tires using neural network,” *Transactions of the Japan Society for Aeronautical and Space Sciences*, 41 (131), 1998, 29-37.
5. Al-Garni, A.Z. "Neural Network-Based Failure Rate of Boeing-737 Tires," *AIAA – Journal of Aircraft*, Vol. 34, No. 6 (1997), pp.771-777 (1417 H)
6. Al-Garni, A.Z., Jamal, A., Saeed, F., & Kassem, A.H. “Failure rate analysis of Boeing 737 brakes employing neural network,” *Proceedings of the 7th AIAA Aviation Technology, integration, and Operations (ATIO) Conference*, Belfast, Northern Ireland, 2007.
7. A. Z. Al-Garni, “Comparison of Aircraft Tire Replacement Policy at Saudi Aviation Facility to the International standards,” *Journal of Quality in Maintenance Engineering*, Vol. 2, No. 4 (1996), pp.71-80 (1416H).

8. Al-Garni, A.Z., Sahin. And Al-Farayedhi, A.A., "A Reliability Study of Fokker F-27 Airplane Brakes", *Reliability Engineering and System Safety*, Vol.56, pp.143-150, 1997.
9. Al-Garni,A.Z., Ahmad Jamal, Abid M. Ahmad, Abdullah M. Al-Garni, and Mueyyet Tozan., "Failure-Rate Prediction for De Havilland Dash-8 Tires Employing Neural-Network Technique", *Journal Of Aircraft*, Vol. 43,2006, 537-543.
10. Al-Garni, A.Z., and Ahmad Jamal., "Artificial Neural Network Application of Modeling Failure Rate For Boeing 737 Tires", *Journal Of Aircraft*, Vol. 34, 1997, 771-777.
11. Al-Garni, A.Z., Sahin, A.Z., Al-Ghamdi, A.S and Al-Kaabi, S.A., "Reliability Analysis of Aeroplane Brakes", *Quality and Reliability Engineering International*, Vol.15, pp. 143-150, 1999.
12. Al-Garni, A.Z., Tozan, M., Al-Garni, A.M. and Jamal, A., "Failure Forecasting of Aircraft Air-Conditioning/Cooling Pack with Field Data", *AIAA Journal of Aircraft*, Vol. 44, No. 3, pp. 996-1002, (2007).
13. Tozan, M., Al-Garni, A. Z., Al-Garni, A. M. and Jamal, A., "Failure Distribution Modeling for Planned Replacement of Aircraft Auxiliary Power Unit Oil Pumps", *Maintenance Journal*, Vol. 19, No. 1, pp. 60-69, (2006).
14. Sheikh A, Younas M, Al-Anazi, D., "WEIBULL ANALYSIS OF TIME BETWEEN FAILURES OF PUMPS USED IN AN OIL REFINERY", *The 6th Saudi Engineering Conference, KFUPM, Dhahran, 2002*, Vol. 4, pp 475-491.

15. Samaha, M. E., Oct. 1997, "Effective utilization of equipment failure history through Computerized maintenance management system," *ASME-ASIA '97 Congress and Exhibition*, pp. 2-8.
16. Erwin V. Zaretsky, Robert C. Hendricks, and Sherry Soditus, "Weibull-Based Design Methodology for Rotating Aircraft Engine Structures", *International Journal of Rotating Machinery* Volume 9 (2003), Issue 5, Pages 313-325.
17. Lewis, E. E., 1987, *Introduction to Reliability Engineering*, John Wiley & Sons.
18. R. B., 1996, *The New Weibull Handbook*, Gulf Publishing Co., pp.2-3.
19. McCulloch, W. S. and Pitts, W. H. (1943). A logical calculus of the ideas immanent in nervous activity. *Bulletin of Mathematical Biophysics*, 5:115-133.
20. Hebb, D. O. *Organization of behavior*. New York: Wiley, 1949.
21. Rosenblatt, Frank. *The Perception: A Probabilistic Model for Information Storage and Organization in the Brain*, Cornell Aeronautical Laboratory, *Psychological Review*, Vol. 65, No. 6, pp. 386-408.
22. Widrow, B. and Hoff, M. (1960). Adaptive switching circuits. In *Western Electronic Show and Convention, Volume 4*, pages 96-104. IEEE.
23. J. J. Hopfield, "Neural networks and physical systems with emergent collective computational abilities", *Proceedings of the National Academy of Sciences of the USA*, vol. 79 no. 8 pp. 2554-2558, April 1982.

24. Parker, D. (1985). Learning logic, "Technical Report TR-87," Cambridge, MA: Center for Computational Research in Economics and Management Science, MIT.
25. Kutsurelis, Jason E. "Forecasting Financial Markets Using Neural Networks: An Analysis Of Methods and Accuracy" United States Navy Post Graduate School, September 1998.
26. Soumitra Paul. "Application of Artificial Neural Networks in Aircraft Maintenance, Repair and Overhaul Solutions" Total Engineering, Analysis and Manufacturing Technologies conference, 22-24 September 2008.
27. Abd Kadir Mahamad, Sharifah Saon, Takashi Hiyama. "Predicting remaining useful life of rotating machinery based artificial neural network" Computers & Mathematics with Applications, Vol. 60, pp.1078-1087, August 2009.
28. Sivanandam, S.N., Sumathi, S., Deepa, S.N., "Introduction to Neural Networks Using Matlab" McGraw-Hill, New York, NY, 2006.
29. Ebeling, C.E., "An Introduction to Reliability and Maintainability Engineering", McGraw-Hill, New York, NY, 1997.
30. Demuth H, Beale M., Neural Network Toolbox, The Math Works.
31. Paul A. Tobia; David C. Trindade, "Applied Reliability" *Sun Microsystems, Inc., Palo Alto, California, USA.*
32. Johnson, Leonard G., "The Median Ranks of Sample Values in their Population With an Application to Certain Fatigue Studies," Industrial Mathematics, Vol. 2, 1951.

33. Haykin, *Neural Networks, a comprehensive foundation* (Englewood Cliffs, NJ: Prentice-Hall, 1999).
34. Lawrence L. Lapin, “Modern Engineering Statistics” Thomson, 1996.
35. Y. Yoon and G. Swales. Predicting stock price performance: A neural network approach. In *Neural Networks in Finance and Investing*, chapter 19, pages 329–342. Probus Publishing Company, 1993.
36. Mann, N., R. Schafer, and N. Singpurwalla “Methods for Statistical Analysis of Reliability and Life Data”, John Wiley, NY, 1974.
37. Saudi Aramco, “Boeing 737 Flight Operation Manual” Vol. 1, 2008.

VITA

Mr. Waheed Al-Wadiee was born in Saudi Arabia in 1980. He joined King Fahad University of Petroleum and Minerals at Dhahran in 1998 for Bachelor Degree in Mechanical Engineering, sponsored by Saudi Aramco. He graduated in 2002 and joined the Mechanical Shops Services Department at Saudi Aramco. In 2004, he joined University of North Dakota at United States of America to be a commercial pilot. He is still working as an aircraft pilot with Saudi Aramco. He joined KFUPM as a part-time graduate student in 2006 for his Master Degree in Aerospace engineering.

During his career, he had attended and completed couple of courses and seminars at the following areas:

- Human factors in aviation safety.
- Aviation internal auditors (IATA).
- Flight data analysis (Cranfield University, UK).
- Leadership and management challenges.

Nationality : Saudi

Permanent Address : P.O.BOX 6331, Dhahran 31311, Saudi Arabia

Telephone Number : +96638774882

Email : alwadiee@gmail.com

